CHAPTER - III

MATERIALS AND METHODS

In India, draught animals are important source of farm power but are not utilised for more than 100 days in a year. As the draught animals remain idle for most of the time it is becoming an economic burden on the farmers. The animals may be made more useful by utilising their idle time in other agricultural operations. This will reduce expenditure by farmers on commercial fuels (diesel and electricity) and make animals more useful for farmers as well as for environment.

Present chapter describes identification, development and performance evaluation of matching gadgets through laboratory simulation set up and the performance evaluation of selected matching gadgets with camel powered rotary transmission system.

3.1 Identification of matching gadgets for rotary transmission system

Identification of matching gadgets was done on the basis of requirement of local region and power requirements of each gadget. The gadgets with a power requirement less than 1hp were selected for testing trials in laboratory simulation setup of rotary mode transmission system.

Electricity generation and battery charging in rural region is a great challenge since rural electrification is not completed successfully till now. For this purpose electricity generation system for battery charging was developed by using automobile alternator.

In the Mewar region of Rajasthan main cultivated crop is Maize. But maize dehusking and shelling is a complicated job. There is no such type of maize dehusker and sheller is available which can be operated through rotary mode transmission system. An axial flow type manual operated maize dehusker and sheller available with AICRP on ESA, Udaipur was identified and modified which could be successfully operated through rotary mode transmission system.

Groundnut is one of the most important oil seed crop which is largely cultivated in many regions of Rajasthan and Gujarat. Manual hand decortications are very inefficient and tough job. Mainly batch type oscillating decorticator is popular for groundnut decortications which has a very low output. So rotary drum type continuous groundnut decorticator was identified and modified which could be operated through rotary mode transmission system.

Air compressor is a very important machine which is used in number of operations in rural region. For this purpose small air compressor was identified and it was modified for rotary mode transmission system.

Performance evaluation of identified gadgets was done initially in laboratory conditions for operating at different operating parameters. The details of laboratory simulation setup are described below.

3.2 Laboratory simulation setup

Selection and standardization of different matching gadgets for rotary mode is a very difficult job. Evaluation of the matching gadgets in different conditions cannot be done in rotary mode transmission system. To overcome these problems a laboratory simulation setup for rotary mode was developed. Fig 3.1(a, b, c) indicate different components of laboratory simulation set up and Fig. 3.1(d) shows the schematic diagram of laboratory simulation setup. In this setup all the matching gadgets could be tested in controlled laboratory condition. A 3 hp, three phase variable speed AC induction motor attached with a variable frequency drive and an electrical power meter were used. In this setup different operating rpm for the matching gadgets could be set and corresponding electrical load for that condition was displayed in electrical power meter.

Different components of laboratory simulation setup are follows:

3.2.1 Variable frequency drive AC motor

The motor used in a VFD system is a three-phase induction motor. Various types of synchronous motors offer advantages in some situations, but induction motors are suitable for most purposes and are generally the most economical choice. Certain enhancements to the standard motor designs offer higher reliability and better VFD performance. Controlling the speed of three phase ac motor was done by controlling the frequency of the power line supply, since the motor was synchronized with the line frequency [Fig. 3.1(c)].

3.2.2 Variable frequency drive controller

Variable frequency drive controllers [Fig. 3.1(a)] are solid state electronic power conversion devices. The design first converts AC input power to DC intermediate power using a rectifier or converter bridge. The rectifier is usually a three-phase, full-wave-diode bridge. The DC intermediate power is then converted to quasi-sinusoidal AC power using an inverter switching circuit. The inverter circuit is the most important section of the VFD, changing DC energy into three channels of AC energy that can be used by an AC motor. These units provide improved power factor, less harmonic distortion, and low sensitivity to the incoming phase sequencing than older phase controlled

(a) Variable frequency drive controller

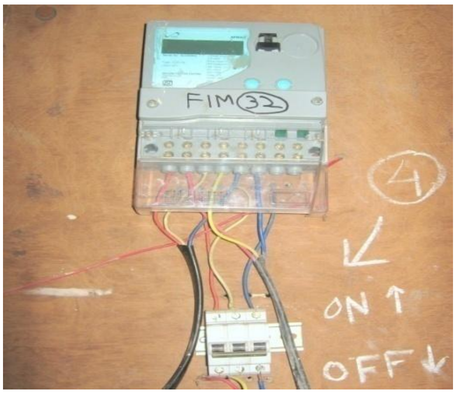

(b) Energy meter **(c) Variable frequency drive motor**

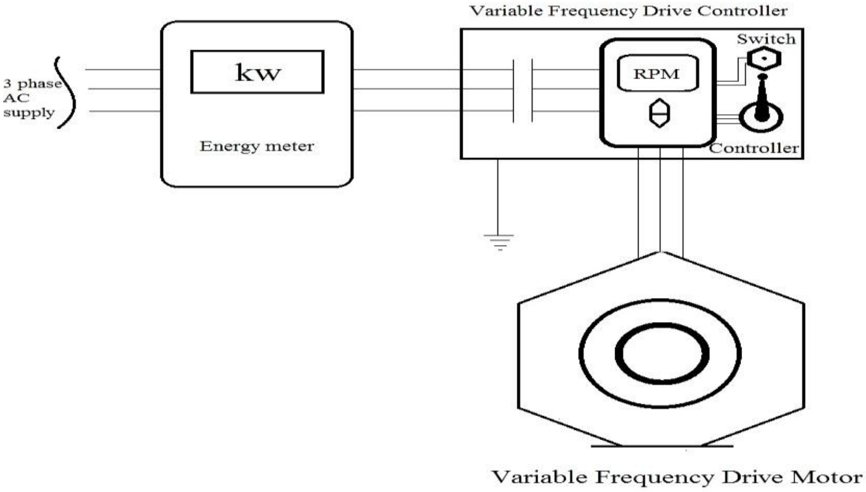

(d) Schematic diagram of laboratory simulation setup

Fig. 3.1: Different components and symmetric diagram of laboratory simulation setup

converter VFD's. As new types of semiconductor switches had been introduced, these have promptly been applied to inverter circuits at all voltage and current ratings for which suitable devices are available. AC motor characteristics require the applied voltage to be proportionally adjusted whenever the frequency is changed in order to deliver the rated torque. For example, if a motor was designed to operate at 460 volts at 60 Hz, the applied voltage must be reduced to 230 volts when the frequency was reduced to 30 Hz. Thus the ratio of volts per hertz must be regulated to a constant value (460/60 = 7.67 V/Hz in this case). For optimum performance, some further voltage adjustment is necessary especially at low speeds, but a constant volt per hertz is a general rule. This ratio could be changed in order to change the torque delivered by the motor.

The usual method used to achieve variable motor voltage is pulse-width modulation (PWM). With PWM voltage control, the inverter switch was used to construct a quasi-sinusoidal output waveform by a series of narrow voltage pulses with pseudosinusoidal varying pulse durations. Fig. 3.2 indicates the schematic view of variable frequency drive motor.

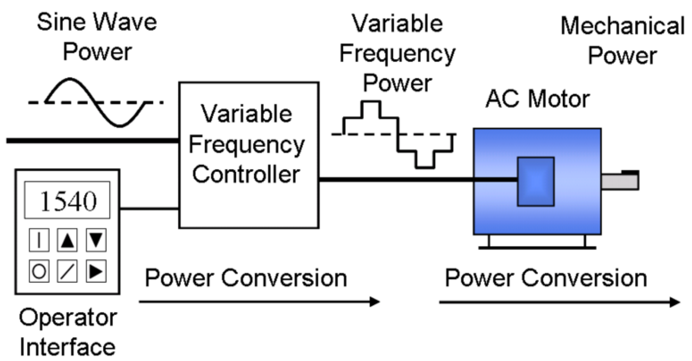

Fig. 3.2: Schematic view of variable frequency drive motor

3.2.3 Energy meter

It is the device [Fig. 3.1(b)] that measures the amount of electric energy consumed by an electrically powered device. With this device the rate of energy consumed was measured. These readings denote the load of a electrically powered device. Electronic meters displayed the energy used on an LCD or LED display, and could also transmit readings to remote places. In addition to measuring energy used, electronic meters recorded other parameters of the load and supply such as maximum demand, power factor and reactive power used etc.

3.3 Development and performance evaluation of identified matching gadgets for rotary mode of transmission system through laboratory simulation setup

Developments of identified matching gadgets were done on the basis that the matching gadgets should not require more than 0.75 kW for continuous work, as camel powered matching gadgets cannot deliver more than 1hp or 0.75 kW for continuous operation. All the gadgets were tested for maximum possible output and efficient operation.

3.3.1 Development of electricity generation system for battery charging

Due to disparity in demand and supply of electric power, mainly for rural areas animal power is under utilization in our country. It is desirable to utilize animal power up to maximum possible extent. One of the ways of utilizing the animal power could be for electricity generation in remote villages in hills or plain areas where either the electric supply is not regular or is erratic to meet the demand of the household for lightening. The electricity generated could be stored in a battery to be used as per the need. On one hand this will make the farmers self sufficient and on the other hand lessen the load on national power supply.

Albeit camels have been used as draught animal for years, not much information is available on physiological behavior of camels in sustained working in rotary mode of operation. Therefore, the present investigation was planned to assess the physiological endurance limit of draught camel in rotary mode of operation for battery charging.

3.3.1.1 Technical consideration for electricity generation by alternator for battery charging:

3.3.1.1a Alternator

An alternator is an electromechanical device that converts mechanical energy to electrical energy in the form of alternating current. Most alternators use a rotating magnetic field. In principle, any AC electrical generator can be called an alternator, but usually the word refers to small rotating machines driven by automotive and other internal combustion engines. In automotive alternator produced AC current are converted to the DC current through rectifier circuit.

Alternators are used in modern automobiles to charge the battery. Alternators have the great advantage over direct current generators of not using a commutator, which makes them simpler, lighter, less costly, more rugged than a DC generator, and the slip rings allow for greatly extended brush life. The stronger construction of automotive alternators allows them to use a smaller pulley so as to turn faster than the engine, improving output when the engine is idling. Alternators use a set of rectifiers (Diode Bridge) to convert AC to DC. To provide direct current with low ripple, alternators have a three-phase winding. In addition, the pole-pieces of the rotor are shaped (claw-pole) so as to produce a voltage waveform closer to a square wave that, when rectified by the diodes, produces even less ripple than the rectification of three-phase sinusoidal voltages. Modern alternators have a voltage regulator built into them. The voltage regulator operates by modulating the small field current in order to produce a constant voltage at the stator output. The field current is much smaller than the output current of the alternator.

Where the brushes in a generator are relatively accessible for service and replacement, the alternator's brushes are not. The alternator must be disassembled to reach and change the brushes. However, the smooth slip rings cause so little brush wear that they may be said to last as long as the life of the alternator.

Efficiency of automotive alternators is limited by fan cooling loss, bearing loss, iron loss, copper loss, and the voltage drop in the diode bridges; at part load, efficiency is between 50-62% depending on the size of alternator, and varies with alternator speed.

3.3.1.1b Charge Termination

Once a battery is fully charged, the charging current has to be dissipated somehow. The result is the generation of heat and gases both of which are bad for batteries. The essence of good charging is to be able to detect when the reconstitution of the active chemicals is complete and to stop the charging process before any damage is done while at all times maintaining the cell temperature within its safe limits. Detecting this cut off point and terminating the charge is critical in preserving battery life. In the simplest of chargers this is when a predetermined upper voltage limit, often called the termination voltage has been reached. This is particularly important with fast chargers where the danger of overcharging is greater.

- **Safe Charging**

If for any reason there is a risk of overcharging the battery, either from errors in determining the cutoff point or from abuse this will normally be accompanied by a rise in temperature. Internal fault conditions within the battery or high ambient temperatures can also take a battery beyond its safe operating temperature limits. Elevated temperatures hasten the death of batteries and monitoring the cell temperature is a good way of detecting signs of trouble from a variety of causes. The temperature signal, or a resettable fuse, can be used to turn off or disconnect the charger when danger signs appear to avoid damaging the battery. This simple additional safety precaution is particularly important for high power batteries where the consequences of failure can be both serious and expensive.

- **Charging Times**

During fast charging it is possible to pump electrical energy into the battery faster than the chemical process can react to it, with damaging results.

The chemical action cannot take place instantaneously and there will be a reaction gradient in the bulk of the electrolyte between the electrodes with the electrolyte nearest to the electrodes being converted or "charged" before the electrolyte further away. This is particularly noticeable in high capacity cells which contain a large volume of electrolyte.

3.3.1.2 Components of developed electricity generator for battery charging:

1. Alternator
2. Frame
3. Pulley system
4. Charging circuit with control panel
5. Battery
6. Direct CFL lightning circuit

3.3.1.3 Determination of battery charging parameters under controlled laboratory conditions

Fig. 3.3 shows the isometric view of electricity generation setup and Fig. 3.4 indicated the schematic diagram of battery charging circuit. It was very difficult to study the battery charging characteristics at wide range of rotational speeds of an automobile alternator with animal operated rotary transmission system therefore; an experimental setup was developed for determining battery charging parameters in laboratory under controlled conditions. Simulation technique was used to create conditions similar to that of animal powered rotary transmission system. Experimental setup consisted of variable speed motor, control panel, alternator, voltmeter, ammeter, energy meter, battery, railings and MS frame (Fig. 3.5).

An automobile alternator of 32 Amp and 12 Volt capacity of Lucas, mounted on power transmission frame was connected to a variable speed motor through V-Belt and pulleys for providing rotational speed. Variable speed motor and power transmission frame were mounted on MS railings. Output of the alternator was connected to the battery terminal through an output variable panel on which ammeter, indicator bulb, on-off switch and sockets for connecting multimeter were provided. The alternator was operated at different speeds by varying the motor rpm through speed controller. Initially experiment was conducted for determining actual rpm of alternator at which alternator starts producing current. After that current, voltage and power were measured at different alternator rpm. Further experiments were conducted at minimum rpm at which alternator starts producing current. Power requirement, current drawn by the battery, charging time, voltage and specific gravity of the battery electrolyte were recorded at regular intervals. On the basis of the results of this experiment the alternator RPM for conducting actual experiments with rotary transmission system was decided.

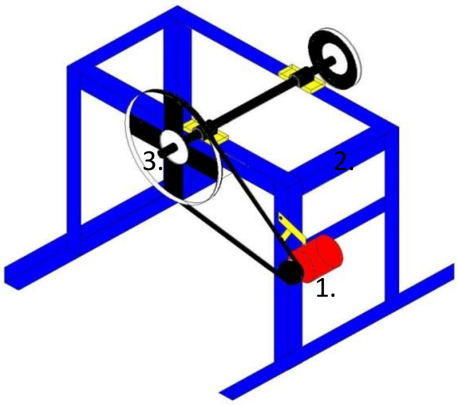

1.	Alternator
2.	Frame
3.	Pulley

Fig. 3.3: Isometric view of electricity generation setup

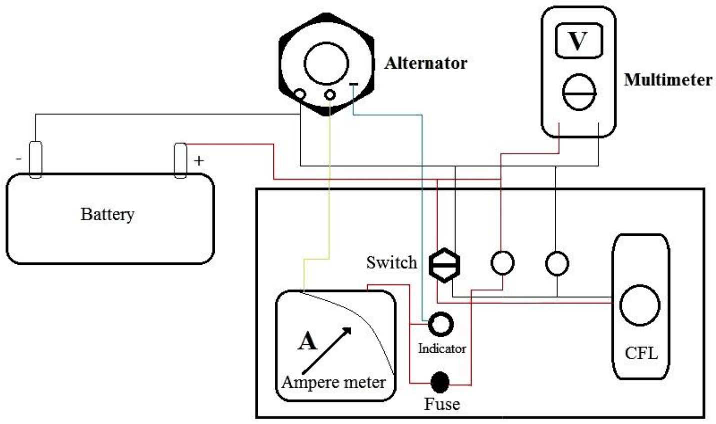

Fig. 3.4: Schematic diagram of battery charging circuit and control panel

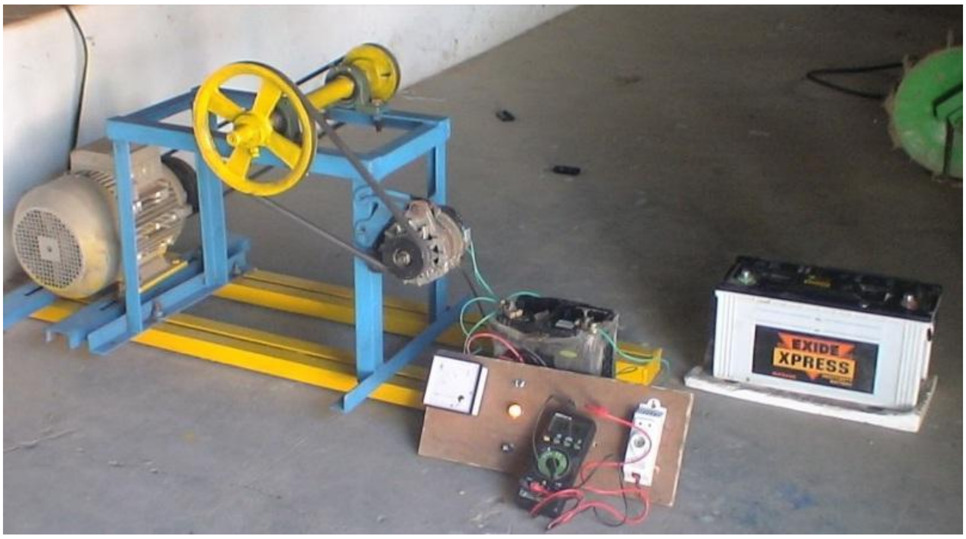

Fig. 3.5: Electricity generator for battery charging in laboratory simulation setup

3.4 Maize dehusker sheller

A manually operated maize dehusker sheller developed by AICRP on ESA, Udaipur center was identified for the study and some modifications in power transmission system were incorporated for operating it through a motor or rotary transmission system. Theoretical considerations and details of design and development are described in following sections.

Theoretical considerations are essential for studying the various aspects involved in development and evaluation process. Hence, the theories on detachment of grain from maize cobs are discussed.

3.4.1 Detachment of grain from maize cobs

Threshing of un-dehusked maize cobs includes removal of the husk as well as separation of grains from the kernels of cobs. Therefore, dehusking and shelling are the two important unit operations for obtaining the maize kernels and removing the outer sheath, heart, stem, etc from the cobs. The dissemination of energy in dehusker-sheller may be considered as an impact process, shear and abrasion. The entire threshing process is considered to be a resultant of a number of impacts whose interval, though not equal, is however fairly regular.

The strength of the bond between the sheath & grain and grain & the kernel depends upon the type and variety of crop, its ripening stage and moisture content. As the moisture content of the grain decreases, the deformation force also follows the same pattern. This is due to the fact that as the moisture content of grain diminishes, the cell contents of the tissue of the abscission layer become hardened due to drying and the cell wall becomes brittle making the detachment easier. The force required and energy consumption is least if applied in the direction where undehusked cob material has least value of strength parameters as strength parameters vary in different directions due to the fibrous structure of the plant material.

Bosoi et al.; (1990) stated that the disruption of bond between the grain and the ear may be static when force is determined necessary for this purpose and dynamic when determines the work done**.** The static method consists of centrifuging. When the ears are centrifuged, the reaction of the bond forces caused by the centrifugal force break these bonds due to the force,

$$P = \frac{G\ r\ \omega^2}{g} \qquad \text{------- (3.1)}$$

Where,

P = force, N

G = weight of the grain, N

r = distance from the axis of rotation to the grain in the ear, m

ω = angular velocity of the centrifuge, rad/s

g = acceleration due to gravity, m /s^2

In the dynamic method, the ear with the grain is subjected to an impact. At impact, the kinetic energy of the grain, m (kg) x v^2 (m/s)/2 is expending in dislodging the grain from the ear. The work done is A (J) = G (N) x h (m). The plant mass entering the clearance between the drum and the concave of a thresher is carried over by beaters and does not hamper the feed of the next portion.

The production capacity (feed rate) is generally expressed by

$$q = \Delta\, \rho\, u_1\, l \qquad \text{------- (3.2)}$$

Where,

q = production capacity (feed rate), kg/s

Δ = thickness of plant mass layer at the entrance to the thresher, m

ή = coefficient designating the utilization of the drum length

ρ = density of the plant mass, kg/m^3

u_1 = velocity of the plant mass entering the thresher, m/s

l = length of the drum, m

The thresher does not become clogged if the beater imparts an impulse force (PΔt) to the fraction of the plant mass, i.e.

$$P\, \Delta\, t \geq m'\, u_1 \qquad \text{------- (3.3)}$$

It indicates that the impulse force should be greater than momentum. The impulse force imparted by the drum to the portion of the plant mass is given by the equation:

$$P\, \Delta\, t = \left(f_1\, N - f_2\, N\right) \Delta\, t \geq m'\, u_1 \qquad \text{------- (3.4)}$$

Where,

N = normal compressive force, N

f_1N = frictional force that appears at the zone of contact between the beater on the drum and plant mass along the tangent to the drum in the direction of its rotation

f_2N = frictional force that appears at the zone of contact between the plant mass and the plates on the concave opposite to that of the plant mass.

f_1 and f_2= coefficients of friction between the plant mass and the beater and concave

Δt = duration for which a beater strikes the portion of plant mass,

s = (b/v)

b = working width of the beater, m

v = peripheral speed of drum, m/s

m' = plant mass to be fed, kg-m/s

= (q x t/g)

q = feed rate, kg/s

t = time interval between the passage of two adjacent beaters, s

= (π D/Mv)

D = outer diameter of the drum, m

M = number of beaters on the drum

g = gravitational acceleration, m/s^2

u_1 = velocity of plant mass entering the thresher, m/s

Then

$$N\left(f_1 - f_2\right)\frac{b}{v} \geq \left(\Delta\,\eta\,\rho\,l\right)$$

Let us determine u_1 from equation 3.3 and substitute in $N(f_1\text{-}f_2)\,(b/v) \geq (\Delta\ \eta\ \rho l)$, that is,

$$N\left(f_1 - f_2\right)\left(b\right) \;\geq \frac{q^2\,\pi\,D}{\Delta\,\eta\,\rho\,l\,g\,M}$$

From which,

$$q \leq \sqrt{\frac{N\left(f_1 - f_2\right) b\,\Delta\,\eta\,\rho\,l\,g\,m}{\pi\,D}}$$

Let a factor of compression β = Δ/δ for plant mass in the thresher clearance and to shift the plant mass in the concave of the beater without any interruptions and clogging, β must not exceed its critical value (β_k). The magnitude of β_k depends upon the physical and mechanical properties of the crop being threshed.

Considering that Δ = β δ,

$$q \leq \sqrt{\frac{N\left(f_1 - f_2\right) b\,\beta\,\delta\,\eta\,\rho\,l\,g\,m}{\pi\,D}} \qquad \text{------- (3.5)}$$

It is assumed that the plant mass passes through the thresher clearance at a constant average speed and some specific thickness. Thus, the forces which govern the process of threshing and separation over the entire angle of contact remain invariant with time. Consequently, the greater the amount of unthreshed grain, the greater is their number under threshing at any given time.

Let,

x = number of un-threshed grain in concave
y = number of threshed and free grains in the concave
z = number of grains passing through the concave grating

For any time interval of plant mass motion expression x + y + z = X (Constant is valid)

During threshing, the number of unthreshed grain decreases and the rate of decrease may be logically represented as a function of the number of unthreshed grain:

$$\frac{dx}{dt} = -\,\beta\,x$$

Where,

β = proportionality constant, 1/s

Similarly, the rate of grains threshed by

$$\frac{dz}{dt} = \gamma\ y$$

Where,

γ = proportionality constant, 1/s

Then the rate of change of free grains, remaining in the concave is

$$\frac{dy}{dt} = \beta\ x - \gamma\ y$$

Magnitude of βx is indicated as positive since it represents an increasing rate for the number of threshed grains.

Change in the state of the total number of grains X can be expressed by the set of differential equations,

$$\frac{dx}{dt} = -\ \beta\ x; \qquad \frac{dy}{dt} = \beta\ x - \gamma\ y; \qquad \frac{dz}{dt} = \gamma\ y \qquad \text{------- (3.6)}$$

The first expression ($dx/dt = -\ \beta x$) in this equation, independent of others, is a linear differential equation with separable variables and further transforms to

$$\frac{dx}{x} = -\ \beta\ dt$$

whose integration gives

$$In\ x = -\ \beta\ t + c$$

Where, c = constant of integration.

Assuming that the constant of integration $c = \text{In}\ c_1$, then

$$In\ x = -\ \beta\ t + In\ c_1$$

or

$$In\left(\frac{x}{c_1}\right) = -\ \beta\ t\ ; \qquad \left(\frac{x}{c_1}\right) = e^{-\beta t} \quad \text{and} \quad x = -\ \beta\ t + c$$

The constant c_1 is evaluated by applying the initial conditions, at $t = 0$, $x = X$

Hence,

$$c_1 = X$$

the value of c_1 is put in $x/c_1 = e^{-\beta t}$ and the expression finally becomes

$$x = Xe^{-\beta t}$$

The second differential equation of 3.6 ($dy/dt = \beta x - \gamma y$) may be rearranged as

$$\frac{dy}{dt} + \gamma\, y = \beta\, x$$

putting the value of $x = Xe^{-\beta t}$ the equation becomes,

$$\frac{dy}{dt} + \gamma\, y = \beta\, X\, e^{-\beta t} \qquad \text{------- (3.7)}$$

This equation being a heterogeneous linear differential equation of the first order that has to be integrated by parts.

By introducing a new variable $y = uv$ and $dy/dt = v\,(du/dt) + u\,(dv/dt)$.

Substituting this in equation 3.7,

$$v\,\frac{du}{dt} + u\,\frac{dv}{dt} + \gamma\, u\, v = \beta\, X\, e^{-\beta t}$$

$$v\left(\frac{du}{dt} + \gamma\, u\right) + u\left(\frac{dv}{dt}\right) + \gamma\, v = \beta\, X\, e^{-\beta t} \qquad \text{------- (3.8)}$$

Assuming that $\left(\dfrac{du}{dt} + \gamma\, u\right) = \mathbf{0}$

$$\left(\frac{du}{u}\right) = -\gamma\, dt$$

$$In\, u = -\gamma\, t + In\, c_1$$

$$In\,\frac{u}{c_1} = -\gamma\, t \qquad or \qquad u = c_1\, e^{-\gamma\, t}$$

Substituting the value of u in equation 3.8,

$$c_1\, e^{-\gamma\, t}\left(\frac{dv}{dt}\right) = \beta\ X\ e^{-\beta\, t}$$

$$\left(\frac{c_1}{e^{\gamma\, t}}\right)\frac{dv}{dt} = \beta\ X\ e^{-\beta\, t}$$

$$dv \;= \frac{\beta\ X}{c_1}\, e^{-\beta\, t+\gamma\, t} \quad , \quad dt = \frac{\beta\ X}{c_1}\, e^{\,t(\gamma-\beta)}\ dt$$

Integrating the above expression,

$$v \;= \left[\frac{\beta\ X}{c_1}\,(\gamma-\beta)\right] e^{\,t(\gamma-\beta)} + c_2$$

Determining y by substituting the values of u and v

$$y \;= \left[\frac{c_1\,\beta\ X}{c_1\,(\gamma-\beta)}\right] e^{(\gamma\, t-\beta\, t-\gamma\, t)} + c_1\ c_2\ e^{-\gamma\, t}$$

or, $$y \;= \left[\frac{\beta\ X}{(\gamma-\beta)}\right] e^{(-\beta\, t)} + c\, e^{-\gamma\, t}$$

where,

c = integration constant that can be evaluated from the initial conditions at t = 0, y = 0,

hence,

$$y \;= \left[\frac{\beta\ X}{(\gamma-\beta)}\right]\left(e^{(-\beta\, t)} - e^{-\gamma\, t}\right)$$

Substituting the above expression in the third differential equation (dz/dt = γy) of 3.7,

$$\frac{dz}{dt} \;= \left[\frac{\gamma\ \beta\ X}{(\gamma-\beta)}\right]\left(e^{(-\beta\, t)} - e^{-\gamma\, t}\right)$$

and integrating the equation after substituting the value,

$$z \quad = \left[\frac{\gamma\,\beta\,X}{(\gamma-\beta)}\right]\left(\frac{e^{(-\beta t)}}{\beta}+\frac{e^{-\gamma t}}{\gamma}\right)+c$$

At t = 0, z = 0 and c = [γ βX/ (γ-β)] (1/ γ - 1/ β),

then

$$z=\left[\gamma\,\frac{\beta\,X}{(\gamma-\beta)}\right]\left(\frac{\left(e^{-\gamma t}\right)}{\gamma}-\frac{e^{-\beta t}}{\beta}-\frac{\mathbf{1}}{\gamma}+\frac{\mathbf{1}}{\beta}\right)=\left[\frac{X}{(\gamma-\beta)}\right]\left(\beta\,e^{-\gamma t}-\gamma\,e^{-\beta t}-\beta+\gamma\right)$$

finally,

$$Z=\frac{X}{\gamma-\beta}\left[\beta\left(e^{-\gamma t}-1\right)-\gamma\left(e^{-\beta t}-1\right)\right] \qquad \text{------- (3.9)}$$

Power intake of the thresher drum is expended on imparting velocity to the plant mass and to overcome the resistance encountered by it during its motion over the concave. Basic equation for impulse force when plant mass is brought into motion, peripheral force appears:

$$P_1\,\Delta t=\Delta\,m\,v, \qquad P_1=\left(\frac{\Delta\,m}{\Delta\,t}\right)v=m'\,v \qquad \text{------- (3.10)}$$

Where,

P_1 = resistance force, N

m' = mass delivered per second, kg-m/s = q/g

q = amount of plant mass delivered to the thresher, kg

g = gravitational acceleration, m/s^2

The resistance P_2 encountered by the drum while displacing the plant mass in the clearance may be taken to be proportional to total periphery force P, i.e., P_2 = f P, where f is a proportionality coefficient or grinding coefficient of the plant mass equal to 0.7-0.8.

The total peripheral force P = $P_1 + P_2$

= m' v + fP

$$P\text{-}fP = m' v$$

$$P(1-f) = m' v$$

So,

$$P = \frac{m' v}{1-f}$$

Multiplying v both sides, the power requirement of drum which goes only toward the production process by

$$P\, v = \frac{m' v^2}{1-f}$$

Where, Pv being equal to 75 kg.m/s N_1, the above expression becomes,

$$75\ N_1 = \frac{m' v^2}{1-f}$$

On the other hand, the prime mover (power source) supplies energy to the threshing drum. During acceleration of the drum while idling:

$$75\ N_1 = J\ \omega \left(\frac{d\omega}{dt} \right)$$

Where,

J = reduced moment of inertia of the drum, kg-m^2

ω = angular velocity of the drum, rad/s

(dω/dt) = angular acceleration of the drum, $1/s^2$

In its turn, the drum does the work of threshing and the products of threshing (grains and straw) accumulate energy and hence the above expression becomes,

$$75\ N_1 = J\ \omega \left(\frac{d\omega}{dt} \right) = \frac{m' v^2}{(1-f)} \qquad \text{------- (3.11)}$$

From equation 3.11, the power of the prime mover may be used to impart angular acceleration to the drum due to irregular feed $m^1$and depending upon the feed, the speed v would increase/decrease or the entire power could be used in threshing if the threshing drum speed is uniform.

It would be desirable that the basic equation for the thresher drum might be expressed in differential form which using the amplitude frequency characteristics could help in finding solution of drum dynamics and drum drive.

Assuming that a) the prime mover or the counter shaft runs at a constant speed, that is $\omega_{p.m}$ = constant; b) while analyzing high velocities, the elasticity of shafts and belts is neglected.

According to the d' Alembert principle, the differential equation for high speeds of the thresher drum is,

$$J\ \omega\left(\frac{d\omega}{dt}\right)+B\ \omega^2+M_t+P\ (t)=M_t\ (\omega) \qquad \text{------- (3.12)}$$

Where,

J = moment of inertia of the thresher drum

ω, ($d\omega/dt$) = angular velocity and angular acceleration of the drum

B = coefficient that accounts for the air resistance to rotation of various components

M_t = constant moment due to friction

P (t) = turning moment necessary to thresh the incoming plant mass consisting of the external load which is a function of time t

M_t (ω) = turning moment developed by the v-belt drive which is a non-linear function of ω

The equation 3.12 is a nonlinear equation because of the ω^2 term and the nonlinear function M_t (ω) in it.

To obtain a linearized equation for the motion of drum which can be solved analytically, substituting the nonlinear function M_t (ω) and B ω^2 by the expression

$$M_t\ (\omega)\ =A_1-B_1\ \omega\ ; \qquad M_{a\,r}=I\ \omega-C$$

Then equation 3.12 may be expressed as

$$J\ \omega\left(\frac{d\omega}{dt}\right)+I\ \omega-C+M_t+p\ (t)=A_1-B_1\ \omega$$

After rearranging, the above expression becomes

$$\left(\frac{a\omega}{dt}\right) + (I + B_1)\frac{\omega}{J} + \frac{(M_t - A_1 - C)}{J} + \frac{\mathbf{1}}{J}\ p\,(t) = \mathbf{0}$$

Writing

$$\frac{(I + B_1)}{J} = m \quad ; \frac{(M_t - A_1 - C)}{J} = n^{\mathbf{1}} \quad ; \frac{\mathbf{1}}{j} = i$$

equation will be

$$\frac{d\omega}{dt} + m\,\omega + n^1 + I\ P\,(t) = 0 \qquad \text{------- (3.13)}$$

The solution of linear equation in general is

$$\omega = \left[\omega_{\mathbf{0}} + \left(\frac{n^{\mathbf{1}}}{m}\right)\right] e^{-m\,t} \int_{\mathbf{0}} i\ P\,(t)\,e^{m\,t}\ dt$$

where, ω_o = initial angular velocity of the drum.

The gross power required for operation of the thresher drum consists of the power required to thresh the plant mass (N_1) and the power required to overcome external resistance (N_2), that is, $N = N_1 + N_2$.

$$75\ N_1 = \frac{m'\,v^2}{(1 - f)} \qquad \text{------- (3.14)}$$

$$75\ N_2 = A\,\omega^2 + B\,\omega^2 \qquad \text{------- (3.15)}$$

Where,

m' = mass delivered per second, kg-m/s = q/g

v = peripheral speed of drum, m/s

f = proportionality coefficient or grinding coefficient of the plant mass equal to 0.7-0.8

N_1 = power required to thresh the plant mass, W

N_2 = power required to overcome external resistance, W

$A\omega$ = resistance at the bearings of thresher drum proportional to its angular velocity, $kgf.m.s^2$

$B\omega^2$ = resistance caused by drum imparting a velocity to the surrounding air proportional to the cube of the angular velocity of the drum, kgf.m.s^2.

ω = angular velocity, rad/s

Then,

$$75\ N_1 = \frac{m'\ v^2}{(1-f)} + A\,\omega + B\,\omega^2 \qquad \text{------- (3.16)}$$

Where, for spike toothed threshing drum A= 0.3x10^{-2} kgf.m and B = 0.48 x 10^{-2} kgf.m.s^2

for the rasp bar thresher A= 0.3x10^{-3} kgf.m and B = 0.68 x 10^{-6} kgf.m.s^2

The feed rate of plant mass to the thresher is

$$q = q_0'\ l\ M \qquad \text{------- (3.17)}$$

Where,

q = feed rate, kg/s

q_0' = permissible feed rate, kg/s.

l = length of the beater, m

M = number of beaters

The stalks are placed perpendicular to the axis of rotation of the drum. During first phase, displacement of the grain does not help in its separation but during second phase, favourable conditions are established for grain separation. The equation 3.17 was used to find out the length of beater of cylinder, for given feed rate.

3.4.2 Physical properties of maize cobs

The length, diameter, weight, moisture content, grain-straw ratio and related data of Pratap-5 variety of maize for un-dehusked and dehusked cobs were recorded using scale, vernier caliper and weighing balance. The standard procedure was adopted for measurement. The grain moisture content was measured as per standard technique of oven dry method. The data are given in Table 3.1.

3.4.3 Components of the maize dehusker-sheller

Of cross-flow and axial flow threshing, axial flow system was opted as material passes through the threshing zone between axial flow cylinder and concave several times due to rearward movement in a helical path, rather than making a single pass in cross-flow cylinder. This feature with axial flow threshing system helps in getting more retention time for un-dehusked cobs during continuous feeding. This system consumes low energy because it does not make fine straw in comparison to spike tooth and rasp bar type threshers. Moreover, with dehusker-sheller, there is no need of making straw.

Fig. 3.6 denotes the 3-D diagram of maize dehusker sheller. Threshing cylinder consisted of beaters. Four beaters in cylinder of axial flow system were taken for providing sufficient space to avoid carrying of un-dehusked maize cobs though periphery of threshing cylinder. This may also help in reducing total power requirement in dehusking-shelling. The beater length of cylinder of axial flow maize dehusker-sheller was decided using eq. 3.17.

$$q = q_0' \; l \; M$$

Assumption,

The feed rate (q) was taken as 0.083 kg/s for feeding one by one cob.

Table 3.1: Physical properties of maize cob

Particulars	**Details**
Variety	Pratap 5
Number of cobs	470
Average length of cob including stalk, mm	237.6 (±) 39.68 [90 to 370]
Average length of un-dehusked cob, mm	201.8 (±) 36 [75 to 290]
% of cob having stalk	94.48
Average stalk length, mm	38 (±) 21.88 [5 to 125]
Average weight of un-dehusked cob, g	194.3 (±) 49.2 [70 to 285]
Maize grain/spent cob ratio	0.78
Maximum grain size (l x b x t), mm	12 x 10 x 5
1000 grain weight, g	358.93
Large diameter of dehusked cob, mm	45.3 ± 3.2
Number of grain lines in dehusked cob	10 to 18
Number of grains in dehusked cob	509 (±) 98
Average large diameter of kernel, mm	28.3 ± 2.9 [23 to 34]
Average small diameter of kernel, mm	21.6 ± 2.4 [16 to 27]
Average length of kernel, mm	155.2 ± 29.65 [105 to 215]
Average moisture content of grain, % (w.b.)	14.7 ± 0.5

Note: The values in parenthesis are range.

Permissible feed rate was taken as 0.029 kg/s considering maximum weight of un-dehusked maize cob.

Number of beaters for making cylinder was 4.

Thus, the cylinder length (l) was calculated by,

$$l = \frac{q}{q_0'} M = \frac{0.083}{0.029 \times 4} = 0.715\,m$$

So, the length of the drum was taken 800 mm for higher output.

The diameter of cylinder was kept 280 mm to achieve the peripheral tip speed of cylinder of about 5.5 m/s at a speed of 350 rpm in this prototype. The solid pegs were welded on upper surface of the drum to make cylinder. The drum dia was kept 170 mm. At the centre of the drum, hole of 32 mm was made to weld MS shaft having 32 mm dia and 750 mm length for providing cylinder shaft.

Based on minimum length of cob, number of solid pegs in each row was kept ten to act as threshing element of the machine. The peg spacing on each row was 100 mm thus during rotation, peg spacing of 75 mm is obtained so that even the small cob having length up to 75 mm is dehusked and shelled.

Design of cylinder shaft was done considering torsion combined with bending assuming uniformly distributed load on simple supporting beam. Following formula was used for calculating diameter of cylinder shaft:

$$\frac{\pi\, d^3}{16} = \frac{\sqrt{T^2 + M^2}}{S_{allow}} \qquad \text{------- (3.18)}$$

Where,

d = diameter of cylinder shaft, cm

T = torque on shaft, kg-cm

M = bending moment on shaft, kg-cm

S_{allow} = allowable stress for mild steel shaft, 560 kg/cm^2

Torque on cylinder shaft was calculated using following formula:

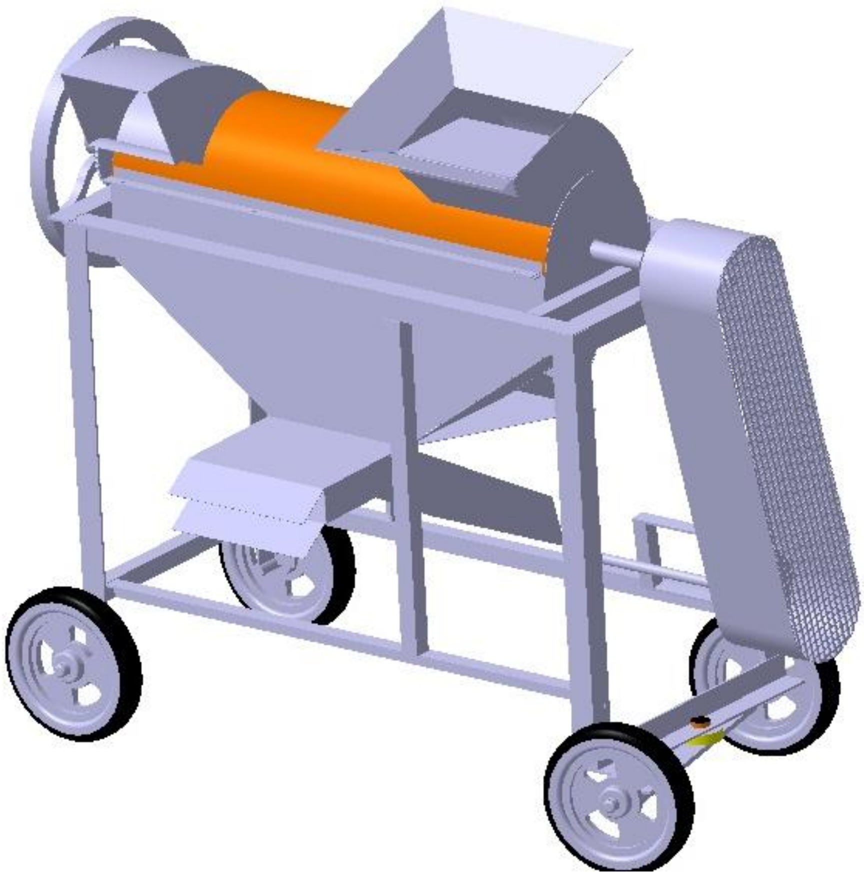

Fig. 3.6: 3-D view of maize dehusker sheller

$$T = \frac{HP \times 4500}{2\,\pi\,N} \qquad \text{------- (3.19)}$$

Where,

HP = horse power to be transmitted, (Considering maximum power that could be developed from rotary mode being of 1.5 hp)

N = speed of shaft, (350 rpm was taken to obtain peripheral speed of 5.5 m/s)

Π = 3.14

Thus,

$$T = \frac{1.5 \times 4500}{2 \times 3.14 \times 350} \quad = 3.07 \text{ kg-m} = 307 \text{ kg-cm}$$

Design torque was kept same as obtained, i.e., 307 kg-cm as maximum power developed by rotary mode being was considered. Bending moment was calculated assuming uniformly distributed load over a simply supported beam. Load was calculated on the basis of cob weight to be fed. Cob weight of 285 g was considered. Assuming load of about two un-dehusked cob (570 g weight), thus, 570 g load will be on cylinder. Bending moment on cylinder shaft was calculated by:

$$M = \frac{W \times l^2}{4} \qquad \text{------- (3.20)}$$

Where,

M = bending moment, kg-m

W = load per metre length, kg/m = 0.57 / 0.725 = 0.786 kg/m

l = cylinder/ main shaft length, m = 1.0 m

$$M = \frac{0.786 \times 1^2}{4} \quad = 0.1965\, kg - m \quad \approx 20\, kg - cm$$

Putting the value of torque, bending moment and allowable shearing stress in equation

$$\frac{\pi\, d^3}{16} = \frac{\sqrt{(307)^2 + (20)^2}}{560}$$

d = 1.409 cm = 14.09 mm = Say 15 mm

Taking 2 as factor of safety, d becomes 30 mm

A 32 mm circular MS shaft of 1000 mm length was taken to accommodate the width of cylinder, cylinder cover, bearings and 100 mm excess shaft to provide driven sprocket. The shaft was stepped down at both ends to accommodate the pedestal having 30 mm ID.

The concave clearance was decided as per the literature and the diameter of kernel (shelled cob) was also considered which varied from 16 to 37 mm. Hence, the concave clearance was kept 30 mm. The hole size of mild steel mesh/sieve for lower concave was kept about 30-35% more than the maximum length/diameter of maize grain (12 mm) so that grain obtained from the process of dehusking-shelling could easily pass through sieve. Thus, hole size of perforated concave screen was kept 16 mm. The thickness of MS perforated sheet was 3 mm. The diameter of concave perforated sheet was kept 330 mm. Length of this concave was 850 mm.

Cylinder cover was made in cylindrical shape using MS sheet of 1.5 mm thick. A rectangular opening (45 mm width x 50 mm height) from both sides was provided for smooth running of cylinder shaft.

The feeding arrangement of the dehusker-sheller has been the ‘throw-in’ type, where whole cobs are fed through hopper. Feed hopper was designed for feeding at required feed rate. The hopper was made using 1.5 mm thick MS sheet. As per the dimension of hopper, it was welded over the opening provided on the cylinder cover. The height of hopper was kept 330 mm to reduce energy requirement in dehusking-shelling maize cobs. The hopper height from ground was kept 1400 mm.

A trapezium shaped grain collecting system was made using one mm thick MS sheet. The trapezium shaped grain collecting unit was attached with the opening provided in bottom cover for grain after dehusking-shelling. This unit was mounted at an angle of 25^0 from horizontal for free flow of maize grain.

One blower arrangement was also attached at the mouth of grain outlet. Blower helped in proper removal of straw material from the grain. Power was delivered to the blower through chain and sprocket drive from the main shaft.

Trapezium shaped frame was provided for maize dehusker-sheller to provide more stability during operation. The frame was made using 35 x 35 x 5 mm angle iron. The length and height of frame was kept 835 and 950 mm, respectively. Correspondingly, breadth at top and bottom was 610 and 830 mm. An angle of 6.61^0 from top breadth was thus provided at each leg. Same size of MS angle iron was welded across all the member of frame to make rigid frame at 100 mm height from bottom of frame. This space was used for providing a small wheel (120 mm diameter solid wheel) at four corners of the frame which facilitated the machine for easy movement of this machine from one place to another place for short distance. Fig. 3.7 shows the different parts of maize dehusker sheller.

One pulley having the diameter of 6 inches was attached to the shaft. Through V belt this pulley was attached to the pulley of the power output shaft of rotary mode transmission system.

3.4.4 Performance evaluation of Maize dehusker sheller in laboratory simulation setup

Maize dehusker sheller was firstly attached on the adjustable MS sliding track of laboratory simulation setup with specially fabricated clamping arrangement (Fig. 3.8). Then the variable speed motor was connected to drum shaft with the help of V-belt arrangement. By adjusting variable speed controller different drum speed was set with the help of tachometer.

Drum speed (rpm): Drum speed was controlled through adjusting the speed of variable speed motor. All the observations were taken at different drum speeds ranging between 300 rpm to 400 rpm.

Load (kw): at different drum speeds electrical load was taken from the energy meter display. According to consideration maize dehusker sheller was driven between the range of 0.75kw.

The tests were conducted in accordance with procedure and guideline proceeded by the BIS code IS 7052-1973.

The sample of 200gm collected from main grain outlet, sieve overflow for maize crop. The sample of 20gm collected from Bhusa outlet for maize crop. Threshing efficiency, cleaning efficiency and sieve overflow were calculated from the different formulae given below. 25 kg bundles of maize were fed separately into maize dehusker sheller and feed rate in kg/hr was determined for different drum speed (rpm). Grain and husks samples of maize dehusker sheller are shown in Fig. 3.9(a) and Fig. 3.9(b).

The dehusking efficiency, output capacity and power consumption were computed as given below,

Total grain input per time was computed as

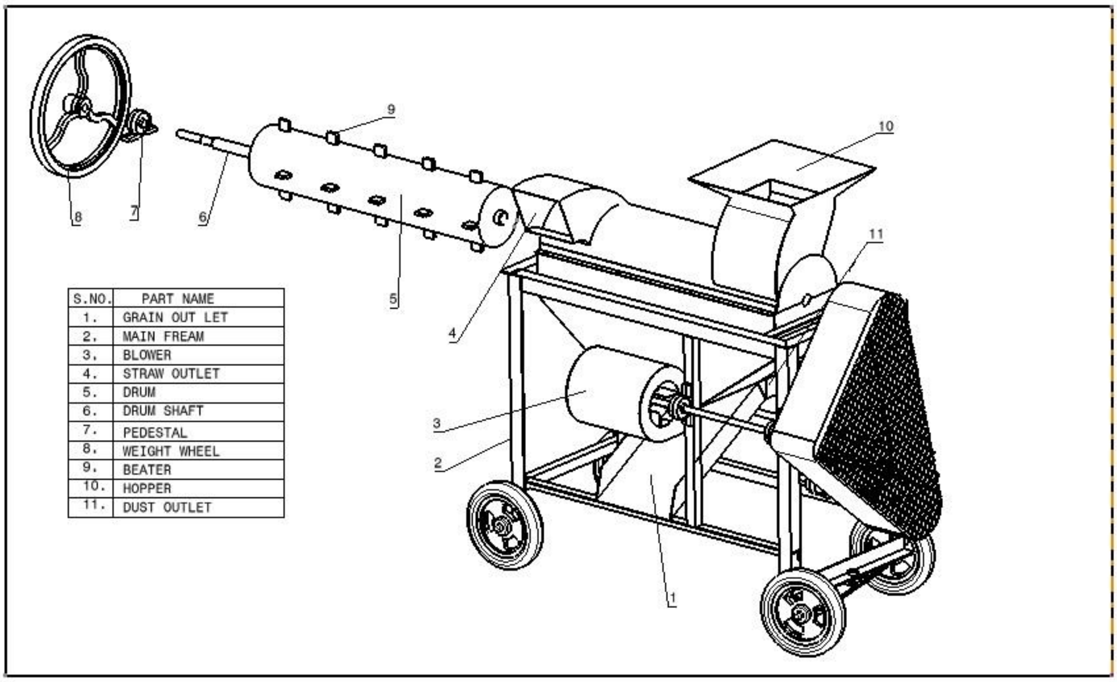

Fig. 3.7: Different components of maize dehusker sheller

Fig. 3.8: Testing of maize dehusker sheller at laboratory simulation setup

(1) A = B+C+D ……(3.21)

Where,

A= total grain input per unit time

B=quantity of clean grain from all outlets per unit time.
C=quantity of broken grain from all outlets per unit time.

D=quantity of unthreshed grain from all outlets per unit time.

(2) Percentage of broken grain =(C/A) x100 ..... (3.22)

(3) Threshing efficiency = (100% of un threshed grain) ..... (3.23)

(4) Cleaning efficiency = (M/F) x 100 % ..... (3.24)

M= Quantity of clean and broken grain obtained from main grain outlet per unit time.

F= Total quantity of sample obtained from main grain outlet per unit time.

(5) Output capacity = Total quantity of threshed grain received at the main grain outlet for test duration and expressed as kg/hr ..... (3.25)

(6) Shelling efficiency = (Wt. of shelled grain)/ (Wt. of total Grain) ..... (3.26)

(7) Dehusking efficiency = {100-(Wt. of husk left on cob)/ (Total Wt. of husk)} x100%

….. (3.27)

3.4.5 Moisture content measurement

The moisture content of maize was calculated from following oven dry method. The crop sample was kept for 24 hrs at 105°C temperature in oven according to IS code7052-1973 and moisture content was calculated accordingly. Fig. 3.9(c) and Fig. 3.9(d) shows the measurement of moisture content of maize sample.

Moisture content of maize crop (in %) = $\{(W_1 - W_2) / (W_1 – W_3)\}$ x100% …. (3.28)

Where,

W_1 =weight of the wet sample in gm
W_2=weight of the dry sample in gm
W_3=weight of the tray in gm

(a) Grain sample (b) Husk sample

(c) Weighing of cob (d) Oven drying of cob

Fig. 3.9: Samples from maize dehusker sheller and measurement of moisture content of maize cob

3.4.6 Grain straw ratio:

Grain straw ratio was calculated by using following formula.

$$Ratio = Wg/ (W_t - W_g) \qquad ..... (3.29)$$

Where,

W_g = weight of grain from sample

W_t = weight of total maize sample

3.5 Groundnut decorticator

The groundnut has a brown soft husk enclosing the kernel in it. The kernels can be separated by cracking the seed coat. This action can be accomplished either by subjecting the pod to impact or by rubbing action. The groundnut is subjected to impact action. The cracking of the seed coat by impact can be accomplished in two ways. One way is to subject the groundnut to impact by a rotating body. In this process the kernel and the husk may be broken into fine particles due to impact forces. There is also a possibility of oozing some oil out of the kernels. This will reduce the efficiency and prevent the separation of husk from the kernels. During the cleaning operation kernels are not suitable for germination purpose. This may spoil the working surface of the machine and consequently will be obstructed.

In other mode of impact seeds are given high rotational forces, results in cracking of the seed coat. The kernel and husks are thus separated due to impact action and fall down in a collecting device but breakage is more. In second method of rubbing action between the grate and rotating shoes results in cracking of seed coat of groundnut. In this case kernels and husks are separated due to shearing force and fall down in a collecting device.

3.5.1 Components of groundnut decorticator

Isometric and schematic diagram of groundnut decorticator are shown in Fig. 3.10 and Fig. 3.11 respectively.

The groundnut decorticator had the following important components:

I. Cylindrical crushing drum
II. Grate
III. Hopper
IV. Flywheel

V. Pulley

VI. Frame

3.5.1.1 Cylindrical crushing drum:

This is the main part of the decorticating unit for decortications of groundnut with the help of grate weighing about 15 kg with the six shoes which is integrated part of the drum (Fig. 3.12). The shoes were made of M.S. flat. The dimensions of the drum were 160 mm diameter and160 mm in length. The numbers of teeth on each shoe were nine. The shoes were mounted on drum made of M.S. flat. The diameter of the cylindrical crushing drum was 160 mm, mounted directly on the transmission shaft. The function of the cylinder was to throw the groundnut pods to the grate.

3.5.1.2 Grate:

This was in the semi-circular shaped fixed below the crushing drum with adjustable clearance of 10 to 30 mm, supported with 4 angle iron pieces of 15 mm x 15 mm x 2 mm fixed on the bottom frame. Due to centrifugal motion of the cylinder in between crushing plate and the grate, the groundnut was crushed and the shell was separated and kernels were fell through the grate. The grate made of M.S. sheet of 20 gauge, had perforation of 10 mm diameter. There was also a provision to move the grate up and down for adjusting the clearance between crushing plate and grate.

3.5.1.3 Transmission Shaft:

The shaft was made of M.S. rod of 25 mm diameter. On the shaft the cylindrical crushing plate was mounted inside the frame with bushes of 35 mm diameter. On the right hand side a fly wheel was fixed with the shaft and on the other side pulley was mounted on the same shaft.

3.5.1.4 Frame:

A prefabricated old cast iron frame was used for holding all the components of groundnut decorticator. Upper rectangular section of the frame having the dimension of 200 mm x 220 mm, the decorticator drum and grate arrangement were attached with that system. Transmission shaft was attached with the frame with the help of pedestal.

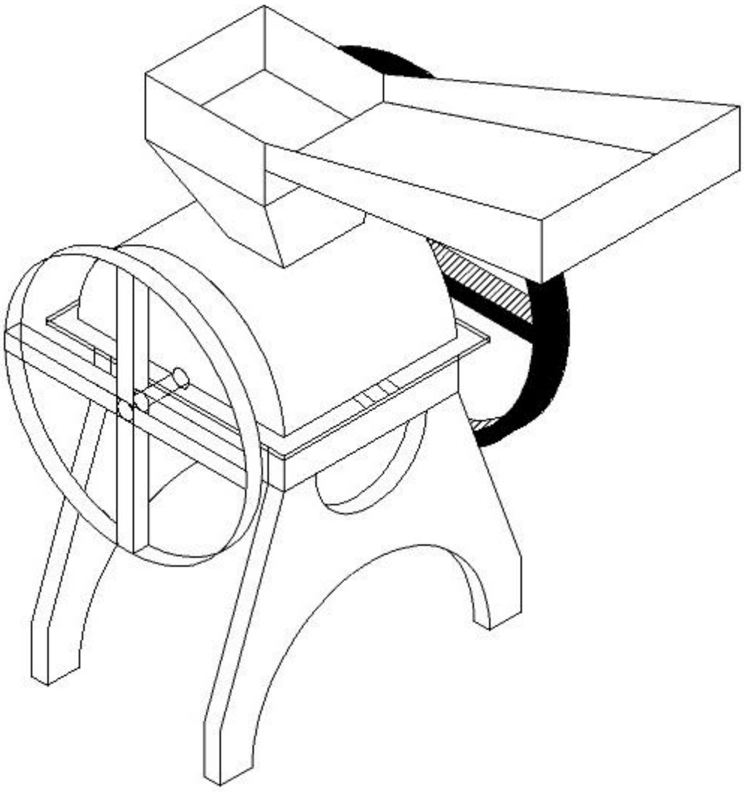

Fig. 3.10: Isometric view of groundnut decorticator

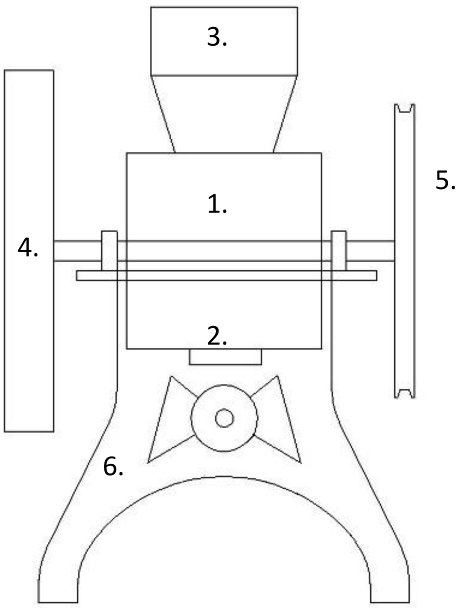

1.	Cylindrical crushing drum
2.	Grate
3.	Hopper
4.	Flywheel
5.	Pulley
6.	Frame

Fig. 3.11: Schematic diagram of groundnut decorticator

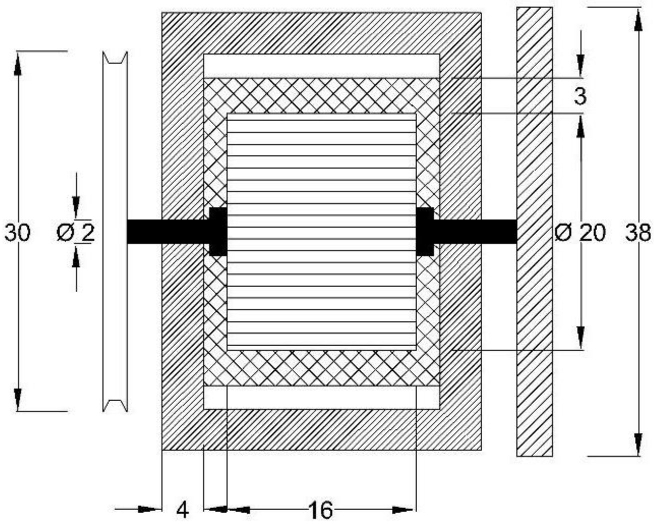

Fig. 3.12: Drum assembly of groundnut decorticator

3.5.1.5 Hopper and drum cover:

Hopper and drum cover is a integrated part and it was made of MS sheet of 20 gauge. Semicircular drum cover having the radius of 120 mm was attached with the frame by nut and bolt arrangement.

3.5.1.6 Flywheel:

Flywheel was selected so as to provide different speeds to check the performance of decortications. The flywheel was made of cast iron of 7 kg fixed on the shaft at right hand side. The diameter of flywheel was 380mm with thickness of 30 mm and a bore of 30 mm. The purpose of the flywheel was to give desired momentum to cylinder for decortications.

3.5.1.7 Outlet:

At the bottom of the machine, beneath the grate, all decorticated pods were collected in a tray. Kernel were separated from the husk manually by winnowing.

3.5.2 Performance of groundnut decorticator in laboratory simulation setup:

Groundnut decorticator was attached on the adjustable MS sliding track of laboratory simulation setup (Fig. 3.13). Groundnut decorticator was tested at different speeds within the ranges of 50 rpm to 400 rpm by adjusting the speed of variable speed motor. Fig. 3.14 shows the different composition of the output of groundnut decorticator.

3.5.2.1 Drum speed: Drum speed was set by regulating the speed of variable speed motor. Drum speed was taken as a independent variable. It was kept in the range of 50 rpm to 400 rpm.

3.5.2.2 Load (kw): At different drum speed, electrical load was recorded from the energy meter display. According to consideration groundnut decorticator was driven between the ranges of 0.75kw.

3.5.2.3 Peripheral speed: Peripheral speed of the cylinder (S) can be given by the formula:

$$S = \pi DN \qquad \text{….. (3.30)}$$

Where,

S = peripheral speed of the cylinder in meter per minute

D = diameter of cylinder in meter

N = revolution of the cylinder per minute.

3.5.2.4 Decortication efficiency: - the decotication efficiency is the ratio of the weight of the decorticated pods to the total weight of decorticated and undecorticated pods, which was calculated by using the following equation.

$$N_d = W_d / (W_d + W_{ud}) \times 100 \qquad \text{….. (3.31)}$$

Where,

N_d = decortication efficiency

W_d= weight of decorticated pods, gm

W_{ud} = weight of undecorated pods, gm

Decortication efficiency is the function of

N_d = f (F, N)

Where,

F = Feed rate

N = Drum speed

Optimum combination of these variables will give maximum efficiency.

3.5.2.5 Broken grain ratio (D):- It is the ratio of weight of broken kernels to the total weight of broken kernels to the total weight of decorticated kernels.

$$D = W_{kb} / W_d \quad \text{..... (3.32)}$$

Where,

D = broken grain ratio

W_{kb} = weight of broken kernels, gm

W_d = weight of decorticated kernels, gm

The kinetic energy by which the speed is striking the grate will vary with the variation in the peripheral speed. By increasing the peripheral speed, the momentum and centrifugal force by which the ground nut pod strikes a hard surface can be increased and its husk can be removed. But excessive increase will cause more damage to the kernels. But in case of hand operated decorticator, at the time of decortications it is better to maintain speed.

3.5.2.6 Moisture content:

Moisture content represents the amount of water present in the pods and it was calculated by using the following formula

$$M = W_w / W_d \times 100 \quad \text{..... (3.33)}$$

Where,

M = moisture content of the ground nut pods in percentage (dry basis)

W_w = weight of water in pods, gm

W_d = weight of dry pods, gm

If moisture content is very low, the pods become brittle and easily decorticated.

3.5.2.7 Feed rate:

Feed rate is the rate of flow of the pods in the cylinder and grate in kg/h the rate of flow will affect the performance. At low rates pods get sufficient surface to strike and become loose. But if feed rate is more, there will be internal sticking between the pods and they will not get sufficient impact by which the husk could be removed. Experiments were conducted at different feed rate for different drum speeds in laboratory conditions for getting optimum feed rate for rotary mode.

Fig. 3.13: Testing of groundnut decorticator in laboratory simulation setup

Fig. 3.14: Constituents of decorticated groundnut

3.6 Air compressor

The function of a compressor is to take definite quantity of fluid and deliver it at a required pressure. Air compressor is used in variety of works in rural sector. A commercially available air compressor of AIRMAX make was identified and selected for the study.

An air compressor takes in atmospheric air, compresses it and delivers the high-pressure air to a storage vessel from which it may be conveyed through the pipeline to wherever the supply of compressed air is required. Since the process of compressing the gas requires that work should be done upon it, it will be clear that a compressor must be driven by some form of prime-mover of the energy received by the compressor from the prime-mover, some will be absorbed in work done against friction, some will be lost due to radiation, and the rest will be maintained within the air itself. The prime-mover converts only a fraction of the heat it receives from the source into work, and as far as the compressor alone is concerned, the energy which it receives is that which is available at the shaft of the prime-mover. Animal driven rotary mode transmission system was used as a prime-mover for air compression in this research context.

3.6.1 Components of air compressor

Air compressor comprised of the following components (Fig. 3.15).

1. Cylinder assembly
2. Valves system
3. Crankshaft and pulley
4. Pressure gauge
5. High pressure hose
6. Safety valve (pressure release valve)

3.6.1.1 **Cylinder assembly**:

Cylinder assembly contains cylinder, cylinder liner piston and connecting rod.

The function of cylinder is to retain the working fluid and to guide the piston. The cylinder made was made of cast iron. Since the cylinder has to withstand high temperature so, fins were provided around the cylinder for efficient air cooling.

Piston is a device which reciprocates within cylinder. Through this air is compressed in the cylinder. Cast iron piston was used for air compressor. Piston clearance was provided for free movement of piston as due to thermal expansion piston size becomes greater than its original size.

Connecting rod delivered thrust from crank shaft to the piston for compression.

3.6.1.2 Valve system:

Inlet valve and outlet valve were used in cylinder head to regulate the movement of air. Cam arrangements were provided to regulate the valve movement according to the different stages of piston movement. At the suction stroke inlet valve remains open and outlet valve remains closed. At the compression stroke inlet valve remains closed and outlet valve remains opened. Inlet valve was attached with a dry type air filter. By high-pressure metallic pipe compressed air was stored in air tank through outlet valve.

3.6.1.3 Crank shaft and pulley:

Crank shaft converts the rotary motion into the reciprocating motion with the help of connecting rod. Crank shaft was immersed in lubricating oil sump. In the outer end of crank shaft pulley was attached for delivering the power from the pulley of rotary transmission system through B-type V-belt.

3.6.1.4 Pressure gauge:

Pressure gauge was attached in the air tank for proper measurement of compressed air pressure. The range of pressure gauge was between 0 to 14 kg/cm^2.

3.6.1.5 High pressure hose:

High pressure hose was attached in air compressor tank through a flow control valve. By this hose compressed air can be used for necessary purpose.

3.6.1.6 Safety valve (pressure release valve):

Safety valve or pressure release valve was used for removal of compressed air if the pressure exceeds the safety limit of 180 lb/in^2.

3.6.2 Performance evaluation of air compressor in laboratory simulation setup:

Air compressor was attached on the adjustable MS railings of the laboratory simulation setup (Fig. 3.16). Air compressor was tested at different crank speeds ranging between 200 rpm to 400 rpm by controlling the motor speed.

3.6.2.1 Crank shaft speed:

Crank shaft speed was taken as an independent variable. Speed of crank shaft was regulated by adjusting the speed of variable speed motor.

3.6.2.2 Time of operation:

Pressure rise in the air tank was directly related to time. With the passage of time the air pressure was pressure rises.

3.6.2.3 Load (kw):

At different crank shaft speeds and time of operation, electrical load was recorded from the energy meter display.

3.6.2.4 Pressure rise (kg/cm^2):

Pressure rise is the prime parameter of air compressor. Pressure rise was observed by the pressure gauge which was attached on the air storage tank.

3.7 Camel Powered Rotary Mode Transmission System

3.7.1 Design of power transmission system

Animal energy can be used in different applications. By making low power electrical generator that can be used for lighting and entertainment equipment such as television and radio as has been done by Kohli (1985). It can also be used as a prime mower to operate maize dehusker cum sheller, groundnut decorticator, battery charging through small alternator, air compressor, centrifugal pumps, thresher, flourmill, oil expeller, cane crushing or small machines of similar nature. The majority of the small machines in villages run between 200 to 2000 rpm. Thus, a device to convert the speed from 2-3 rpm to 200 –2000 rpm can be very useful.

Traditionally single camel is used as power unit for different agricultural or transport operations. So at a time single camel is desirable to operate the rotary mode system, which can

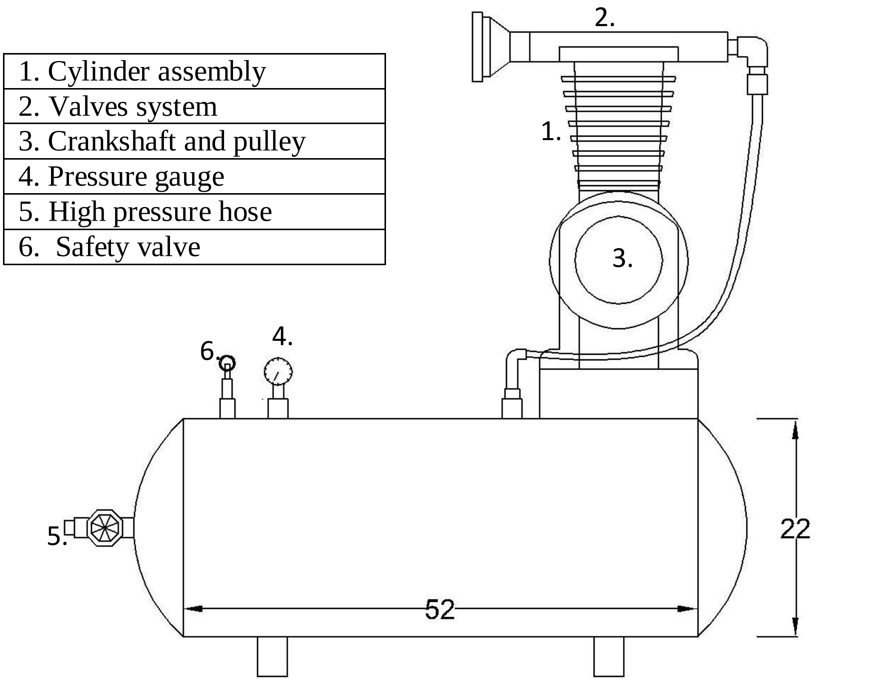

All dimensions are in mm

Fig. 3.15: Schematic diagram of air compressor

Fig. 3.16: Testing of air compressor in laboratory simulation setup

develop 1 kW to operate different agro processing machines. The average speed of bullocks may be taken as 1-1.1 m/s which results in 2-3 rpm on working radius of 3.25-3.75m path.

The design of different elements of power transmission unit is based on the following consideration.

- Normal power that can be developed by a camel is 0.75 kW from safety consideration power that can be generated for a shorter period of time was taken as 1.5 kW.
- The travel speed of the camel is 1.1 m/s

To satisfy the above requirements a gear box was designed which was located at the centre of the animal track. The tractive effort and circular motion of camel was used to operate the system. The system must be efficient, cheap and small in size so that starting inertia is not excessive. Use of gears in animal driven machines like sugarcane crusher, oil expelling and water lifting (Persian wheel) is quite common in past. But all these applications required low speed (5-10 rpm) and high torque. The torque acting on first stage gear is excessive.

3.7.1.1 Calculation of torque

Consider the formula

$$P = \frac{\text{Draught x Velocity}}{1000}$$

Where,

P = Power developed by the camel = 1.5kW

Velocity = 1.1 m/s

Draught comes out to be 1363.5 N or say 1365 N

Draught = Draught developed by the camel in Newton

N = rpm of the camel per minute = 3

Torque acting on the vertical input shaft = Draught x working radius of camel path (3.5m)

= 4777.5 N-m

3.7.1.2 Design of horizontal hitch beam with wheel and operator seat

A horizontal hitch beam was used to transmit power from camel to the vertical input shaft. The beam was fixed to the input shaft through a pin arrangement. This allowed movement of the beam in vertical plane. The beam was a hollow square with internal and external dimensions being 60 and 75 mm, respectively. The length of the beam from the centre of rotation i.e. vertical shaft was 4.5 meter. It resembles a cantilever beam with concentrated load at free end. The safe bending stress for this mild steel section is 75 N/mm^2.

$$F_{max} = \frac{M \, . \, Y_{max}}{I}$$

$$M = \frac{I \, . \, F}{Y_{max}}$$

Where,

M = Bending moment acting on the beam = Draught x length of the beam

= 3071250N-mm

I = Moment of inertia of the beam about the neutral axis

= $[(L_o)^4 - (L_i)^4] / 12$

Where,

L_o = Outer dimension in mm of the section, mm = 75 mm

L_i = Inner dimension of the section, mm = 60 mm

= 1556718.75 mm^4

Y_{max} = Distance of the most distant point of the section from the neutral axis

= 37.5 mm

F_{max} = 73.98 N/ mm^2

The induced bending stress in the mild steel beam of square section is 73.98 N/ mm^2 which is less than the permissible bending stress i.e. 75N/mm^2 (Ramamrutam, 2004). Hence, the design of this beam is safe for this length. It has been reinforced by two mild steel channel section of 75x75 x6 mm to a length of 1.25 m from the vertical input shaft. Total effective length comes out to be 4.5 meter.

3.7.1.3 Design of vertical input shaft

The vertical input shaft is subjected to torsion and torsional stress(**τ_s**) is given by

$$\tau_s = \frac{16T}{\pi d^3}$$

where,

T = torque acting on the shaft = 4777500 N-mm

d = diameter of the shaft = 65 mm

τ_s = 94.99 N/ mm^2

The induced stress in the vertical input shaft is 94.99 N/mm^2 which is less than the permissible yield stress of 353 N/mm^2 for the carbon steel (Mahadevan and Reddy, 1989). Hence, the design of this shaft is safe.

3.7.1.4 Design of crown and pinion

The crown and pinion (Fig.3.17) are spiral bevel gears and are made from heat-treated alloy steel. The specifications for crown and pinion are given below:

- Hardness = 300 BHN
- Surface endurance limit (fes) = 7.70 N/mm^2
- Youngs modulus (E_c and Ep) = 84 kN/mm^2
- Allowable static stress (fs) = 472 N/mm^2
- Pressure angle (p) = 20^o (full depth involved)
- No. of teeth on crown gear (T_c) = 38
- No. of teeth on pinion gear (Tp) = 6
- Face width of crown and pinion (b) = 60 mm
- Module (m) = 12 mm

- Velocity ratio (R) = 38/6 = 6.333
- Pitch circle dia of crown (Dc) = m x T_c = 12 x 38 = 456 mm
- Pitch circle dia of pinion (D_p) = m x T_p = 12 x 6 = 72 mm
- Circular pitch of crown (P_c) = m x π = 12 x 3.14 = 37.7 mm
- Circular pitch of pinion (P_p) = m x π = 12 x 3.14 = 37.7 mm
- Speed of crown (N_c) = 3 rpm
- Speed of pinion (N_p) = N_c.R = 3 x (58/ 6) =19 rpm

Since the pinion is weaker as compared to crown therefore, it was tested for strength and wear consideration. Following factors were considered.

i) Formative no. of teeth on crown (T_{fc}) = [Actual No. of teeth on crown/Cos(α_c)]

Where,

α_c = Semi pitch cone angle of crown

= $\tan^{-1}$(R) = $\tan^{-1}$(6.33) = 81^o 01'

$$T_{fc} = \frac{38}{\text{Cos}\, 81^0 01'}$$

= 243.5 $\cong$ 244

ii) Formative no. of teeth on pinion (T_{fp}) = $\dfrac{\text{Actual No. of teeth of pinion}}{\text{Cos}\,\alpha_p}$

Where,

α_p = Semi pitch cone angle of pinion

= $\tan^{-1}$(1/R) = $\tan^{-1}$(1/6.33) = 8^o 59'

$$T_{fp} = \frac{6}{\text{Cos}\, 8^0 59'}$$

= 6.06 say 7.0

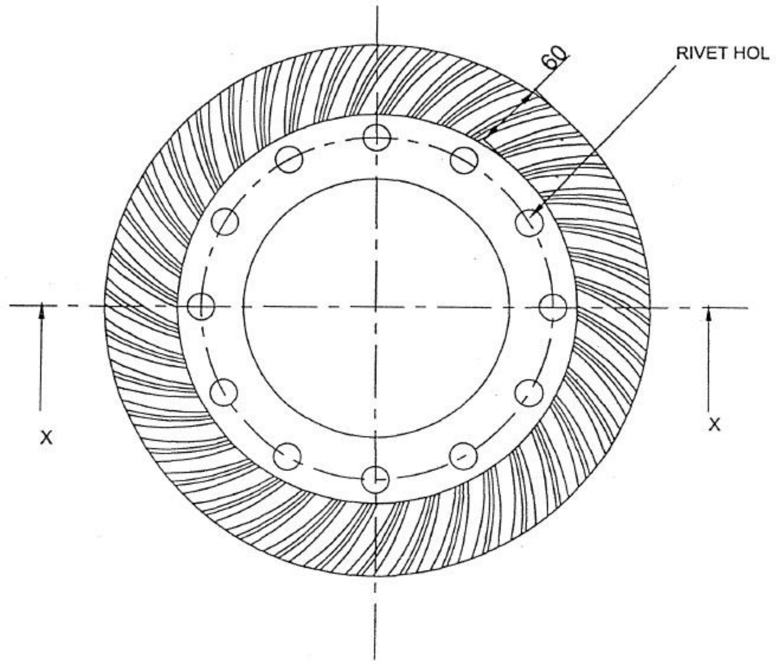

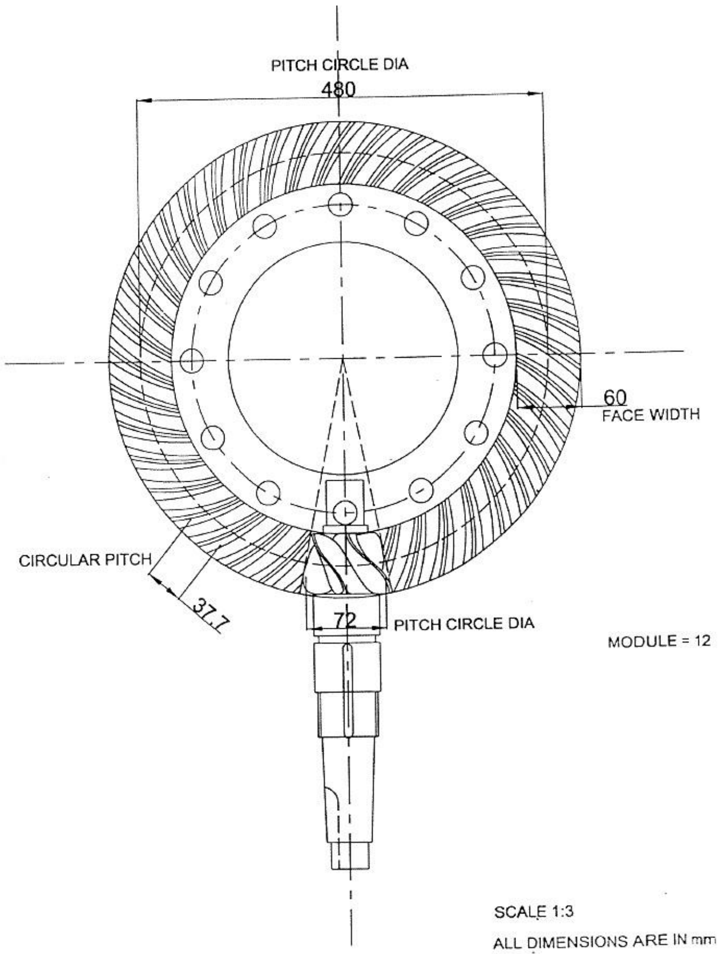

Fig. 3.17: Crown and pinion gear

iii) Form factor for pinion (Y') $= 0.154 - \dfrac{0.912}{T_{fp}}$

$Y' = 0.0237$

iv) Velocity ratio factor (Q) $= 2\dfrac{T_{fc}}{T_{fc} + T_{fp}}$

$= 1.944$

v) Load stress factor (K) $= \dfrac{fes^{2}\ \text{Sinp}\ (1/E_p + 1/E_c)}{1.4}$

$= 3.48$

vi) Pitch line velocity (V_p) $= \dfrac{\pi D_p N_p}{60}$

$= 0.0716$ m/s

vii) Allowable working stress for pinion (fw) can be calculated by assuming the allowable static stress as (fs) = 472 N/mm^2 (Khurmi and Gupta, 1997).

$Fw = fs \times Cvp$

Where $Cvp = \dfrac{3}{3 + V_p}$

$= 0.976$

$Fw = 460.62$ N/mm^2

viii) Length of pitch cone element (L) $= \dfrac{D_p}{2\,\text{Sin}\,\alpha_p}$

$= 230.3$ mm

ix) Bevel factor $= \dfrac{L - b}{L}$

$= 0.757$

3.7.1.5 Design of pinion

i) Permissible wear load (Fw) on teeth of pinion can be calculated as below

$$Fw = \frac{Dp \times b \times Q \times K}{Cos\alpha_p}$$

Where,

Dp = Pitch circle diameter of pinion = 72 mm

B = Face width of pinion = 56 mm

Q = Velocity ratio factor= 1.944

K = Load stress factor = 3.48

α_p = Semi pitch cone angle of teeth = $8^o58'$

Fw = 27616.7 N

ii) The actual tangential load acting on pinion teeth can be calculated as below

$$\text{Torque acting on pinion} = \frac{\text{Torque acting on crown}}{\text{Velocity ratio}}$$

= 754740N-mm

$$\text{Load acting on pinion} = \frac{\text{Torque acting on pinion teeth}}{\text{Pitch circle radius}}$$

Actual tangential load on pinion teeth =20964.98 N

The permissible wear load for pinion teeth is 27616.7N which is higher than the actual tangential load acting on pinion teeth 22467.8N (Khurmi and Gupta, 2005). Hence, the design of pinion is safe.

3.7.1.6 Design of Spur gear and Spur pinion

The spur gear and spur pinion are made from cast steel. The specifications are given below:

- Hardness = 240 BHN

- Flexural endurance limit(fe) = 350 N/mm^2
- Surface endurance limit(fes) = 616 N/mm^2
- Youngs modulus (E_c and Ep) = 84 $x10^3$ N/mm^2
- Allowable static stress (fs) = 196 N/mm^2
- Pressure angle (p) = 14^o 30’ (full depth involute)
- No. of teeth on spur gear(Tsg) = 58
- No. of teeth on spur pinion (Tsp) = 12
- Face width (b) = 40 mm
- Module (m) = 6.0 mm
- Velocity ratio (R) $= \frac{58}{12} = 4.84$
- Pitch circle dia of spur gear (Dsg) = m x T_c 6 x 58 = 348 mm
- Pitch circle dia of spur pinion (D_{sp}) = m x T_p 6 x 12 = 72 mm
- Circular pitch of spur gear (P_{sg}) = m x π 6 x 3.14 = 18.86 mm
- Circular pitch of spur pinion (P_{sp}) = m x π 6 x 3.14 = 18.86 mm
- Speed of spur gear (N_{sg}) = 19 rpm
- Speed of pinion (N_{sp}) = 19 x 4.84 = 91.83 $\cong$ 92 rpm

Since the spur pinion is weaker of the both, it is considered for the design. The design of spur pinion is tested for its strength and wear considerations. Following factors are to be considered.

i) Form factor (Y’) for pinion of 14^o 30’ full depth involute system

$$Y' = 0.124 - \frac{0.684}{T_{sp}}$$

$$Y' = 0.067$$

ii) Velocity ratio factor (Q) for pinion is given by

$$Q = 2\,\frac{R_s}{R_s + 1}$$

$$= 1.657$$

iii) Load stress factor (K) can be calculated as under

$$K = \frac{fes^2\ \mathrm{Sinp}\ (1/E_p + 1/E_c)}{1.4}$$

$$= 1.616$$

vi) Pitch line velocity of pinion is given by

$$V_p = \frac{\pi\, D_{sp}\ N_{sp}}{60}$$

$$= 0.347 \text{ m/s}$$

vii) Allowable working stress for pinion (fw) can be calculated by assuming the allowable static stress for pinion as (fs) = 196 N/mm^2 (Khurmi and Gupta, 1997).

$$Fw = fs \times Cvp$$

$$\text{Where, } Cvp = \frac{3}{3 + V_p}$$

$$= 0.896$$

$$Fw = 175.68 \text{ N/mm}^2$$

3.7.1.7 Design of spur pinion

i) Permissible wear load (Ww) on pinion can be calculated as below

$$Ww = Dsp.\ b.\ Q.\ K$$

Where,

Dsp = pitch circle diameter of pinion = 72

b = face width of pinion = 40 mm

Q = Velocity ratio factor = 1.657

K = Load stress factor = 1.616

= 7711.82 N

ii) The actual tangential load acting on pinion teeth can be calculated as below

$$\text{Torque acting on pinion} = \frac{\text{Torque acting on spur gear}}{\text{Velocity ratio}}$$

= 186799.08 N-mm

$$\text{Load acting on pinion} = \frac{\text{Torque acting on pinion teeth}}{\text{Pitch circle dia of pinion}}$$

Actual tangential load on pinion teeth = 2594.44N

The permissible wear load for pinion teeth is 7711.82N which is (Khurmi and Gupta, 2005) is higher than the actual tangential load acting on pinion teeth 2594.44N. Hence, the design of pinion is safe.

Dynamic tangential tooth load (WD) can be calculated by using Buckingham's equation i.e. WD = WT + WI

Where,

WT = tangential load

WI = increment load due to dynamic action and is given by

$$WI = \frac{21\,V_p\,(b.C + WT)}{21\,V_p + \sqrt{(b.C + WT)}}$$

Where,

b =face width = 40 mm

C= Dynamic load 700 N/mm (Form = 6 the load error is 0.65 for first class gear. Therefore, dynamic load factor C can be taken as 700 N/mm^2

V_p = pitch line velocity of pinion = 0.347 m/s

$$WD = \frac{WT + 21\,V_p\,(b.C + WT)}{21\,V_p + \sqrt{(b.C + WT)}}$$

= 3817.95 N

Considering the tangential stress equation (f_{ind}) on pinion teeth given by Lewis equation

i) $$f_{ind} = \frac{2T_p}{m^3\,.\,K.\,\pi^2\,.\,Y'\,.\,T_{sp}}$$

Where,

T_p = Torque acting on pinion

But torque acting on spur gear = torque acting on bevel pinion

$$T_p = \frac{\text{Torque acting on bevel pinion}}{\text{Velocity ratio}}$$

= 167.5 N-m

m = module = 6 mm

K = Load stress factor = 1.615

Y' = Form factor = 0.067

T_{sp} No. of teeth on pinion = 12

f_{ind} = 121.15 N/ mm^2

Induced tangential stress 121.5 N/mm^2 is less than allowable working stress 175.68 N/mm^2. Hence, the design is safe.

3.7.1.8 Design of Universal Coupling

Universal coupling also known as hooks coupling is used to connect two shafts, which are intersecting at small angle. The end of each shaft is forked to U type and each fork provides two bearings for the arms of a cross. The arms of the cross are perpendicular to each other. The motion is transmitted from the one shaft to another through a cross. The intersection of two shafts may be constant, but in actual practice it varies when the motion is transmitted.

The coupling was made up of mild steel and subjected to torsion. It should be tested for shear stress. The torque after the first stage spur gears is 186799.08 N-mm so the torque after the second stage spur gears will be 186799.08 N-mm/ 4.83 = 38674.6 N-mm. The pin is under double shear and hence the following relation was used.

$$T_{uc} = \frac{2 \text{ x } \pi \text{ x } dp^2 \text{ x } fs \text{ x } ds}{4}$$

Where,

T_{uc} = Torque transmitted through universal coupling = 38674.6 N-mm

dp = diameter of the pin = 38 mm

fs = Induced shear stress in N/mm^2

ds = diameter of the shaft = 38 mm

= 0.45 N/mm^2

The permissible shear stress for mild steel pin is 28 N/mm^2, which is much higher than shear stress induced in the pin (0.45 N/mm^2). Hence, the design is safe.

3.7.1.9 Design of Underground Shaft

The shaft is made up of mild steel and subjected to torsion. It should be tested for shear stress. The torque on the universal coupling was 38674.6 N-mm, which is same for underground shaft

$$\tau_s = \frac{16\, T_s}{\pi\, d_s^3}$$

where,

T = torque acting on the shaft = 38674.6 N-mm

D = diameter of the shaft = 25 mm

= 16 x 38674.6 / [3.14 x (25)^3]

= 12.62 N/ mm^2

The permissible shear stress for mild steel solid shaft is 60 N/mm^2, which is much higher than shear stress induced in the shaft (0.45 N/mm^2). Hence, the design is safe.

3.7.1.10 Design of Ratchet

The material specification of ratchet was same as spur gear and is already discussed in previous section on design of spur pinion. The details of ratchet were as under

No. of teeth on ratchet (T_r)	=	18
Pitch circle diameter	=	180 mm
Module	=	10 mm
Face width	=	10 mm
Circular pitch	=	π m = 31.4 mm

Torque acting on the ratchet (T_R) = $\dfrac{\text{Input torque at vertical input shaft}}{\text{Velocity ratio of the system}}$

= 32302.23 N-mm

Y' = Form factor = 0.1012

K = Load stress factor = 1.616

$$f_{ind} = \frac{2T_p}{m^3 \cdot K \cdot \pi^2 \cdot Y' \cdot T_{sp}}$$

= 7.048 N/mm^2

Induced stress is 7.048N/mm^2 which is less than the allowable working stress of 175.68 N/mm$^{2.}$ Hence, the design is safe.

3.7.1.11 Design of Flywheel

A flywheel is a machine part which may be looked upon as rotating energy reservoir attached to the shaft of particular type of a machine.

The Kinetic Energy of flywheel is given by $E = \frac{1}{2} I\omega^2$

Where,

I = Moment of inertia about the axis of rotation and is equal to $(w/g)\ K^2$

K = radius of gyration

ω = Mean angular speed

$I = m\ r^2$

For an animal drawn power transmission unit energy for a given cycle varies as the camel exerts force on the beam through its limb movement. The flywheel is alternatively absorbing and delivering energy. The speed varies in each revolution as a result flywheel mounted on the shaft is displaced ahead and behind its mean position.

Minimum speed of the flywheel =296 rpm = 30.98 rad /s

Maximum speed of the flywheel =441 rpm = 46.05 rad /s

Power to be transmitted is 1.5 kW

At a mean speed of 368.5 or 370 rpm or 38.52 rad/s

Energy delivered in one pace (400 mm) at an average speed of 3 km/h is 0.4 /0.83= 0.48.

Average energy delivered during this time while the average power generated is 500 W.

1500 x0.48 = 720 Joule

The Kinetic Energy of flywheel is given by $E= ½\ I\omega^2$

I = 0.971 or let 1 $kg.m^2$

I = $½\ M.R^2$

M = mass of the fly wheel

R = radius of gyration of flywheel = 300mm

1 = $M\ (.30)^2$

M = 11.11 kg say

Hence, the weight of flywheel should be more than 11.11 kg.

3.7.1.12 Power Transmission System

The power transmission system converts the animal muscle power to mechanical energy. It mainly consisted of a horizontal hitch beam with wheel and seat for operator, gearbox, universal coupling, shafts, ratchet, flywheel and pulleys. The gearbox was installed inside the circular pit at the centre of the test track. The different components of the unit are described below:

3.7.1.13 Horizontal hitch beam with wheel and operator seat

A horizontal hitch beam of MS square section 75 x 75 mm and length 5.4m was used to transmit the animal power to the vertical input shaft of the gearbox. A seat was provided at outer end of the beam for operator. Pneumatic wheel was also provided at the outer end to support the beam (Fig. 3.18). The position of the seat and the wheel could be changed as per the need of the operator. Inner end of the hitch beam was clamped with the gear unit through a mild steel shaft having diameter of 150mm welded on a circular flange of diameter 225 mm and thickness 10 mm. The flange was bolted to a pin joint, which in turn was welded to vertical input shaft. The pin joint allowed the vertical movement thus preventing the damage to the system due to forces acting on the beam as a result of vertical movement.

3.7.1.14 Gear unit

A gear unit was designed and developed to step up the rpm and to change the direction of motion from the horizontal to a vertical plane. A MS crown gear box (400mm x 400mm x 400mm) was fabricated for mounting different components. A vertical input steel shaft, 65 mm dia and 630 mm long, was mounted on the centre of the gear unit with the help of two thrust bearings (Fig. 3.20). The bearings were encased in cast steel housings. The housings were welded at the inner-top and inner-bottom of the gear box. A crown of a spiral bevel gear (38 teeth) was fixed to the input shaft. A pinion of spiral bevel gear (6 teeth) was meshed with the crown gear. Two ball bearings were enclosed in housing and the pinion was mounted on its position by the bearings. A spur gear of 58 teeth, made up of heat-treated steel was fixed at the other end of the pinion shaft. The spur gear meshed with a spur pinion of 12 teeth mounted on a shaft of 40 mm diameter. The shaft was supported by two pedestal bearings attached to the gear box (Fig.3.19)

On the pinion shaft a oil sump closed gear box was attached. In the second stage gear box similar spur gear with 52 teeth was mounted. This spur gear, in turn meshed with another spur pinion of 12 teeth. The two sets of the spur gear and pinion were so arranged that the final output shaft was parallel and in line with the pinion of bevel gear.

The gear unit was mounted on an MS angle/channel frame which was firmly grouted in the circular pit at the centre of the test track. The output shaft of the second stage spur pinion was connected with the help of two universal couplings, flanges and mild steel shaft of 50 mm diameter to an underground shaft. The universal couplings easily transmitted power at an angle between the output shaft and underground shaft. A MS shaft of 25 mm dia was encased with four ball bearings in a hollow pipe of 100 mm dia buried 200 mm below the test track. The shaft was taken underground so as to avoid any hindrance in the operation. The extreme outer end of the underground shaft and final out put shaft were connected through a ratchet system, provided to cut off the motion to flow backwards and avoid hammering on the legs of the camel when they stop or slow down. The ratchet allows power to be transmitted in one direction only. A Flywheel was mounted on a final output shaft (Fig. 3.20) of 51 mm dia with two sealed pedestal bearings on a MS channel frame grouted by cement concrete. It was provided to maintain inertia and conserve energy of the system. When the camel stopped or slowed down the ratchet divided the system in two parts and thus the entire energy was conserved with the flywheel, which was fully utilised to operate different machines. In absence of ratchet the entire system moved due to inertia of the flywheel thereby unnecessarily reducing the efficiency of the system. The final output was taken through pulley/sprocket fixed to the output end of the underground shaft.

3.7.1.15 Hitching arrangement

Harnessing system plays a very important role in utilising the available animal power efficiently. Two hollow pipes pull beams were used for hitching the animal. Bushes made of hollow pipe were provided at the ends of the pull beams. A swingle tree made of hollow pipe was inserted in these bushes for providing movement in the vertical plane. Further this swingle tree was attached with a horizontal hitch beam through a turntable arrangement to facilitate swinging movement of the pull beams in the horizontal plane. The yoke was supported by the withers and provided the necessary tractive force (Fig. 3.21).

3.7.2 Test track

Test track was a circular piece of land of 6 m radius. It was enclosed in a masonry boundary wall of 300 mm height as shown in Fig. 3.23. The soil was well compacted levelled and cleaned to remove any stone *etc* in the path of the bullocks. The entire track was raised by 20 cm from adjacent land. Openings were provided at certain distance in the circular boundary to drain out the rainwater. At the centre of the track a circular pit of 1200 mm depth and 2000 mm diameter with a masonry wall of 200 mm width all along its periphery was constructed. The gear unit of the developed power transmission unit was mounted on a MS angle frame firmly grouted by cement concrete mortar (Fig. 3.24).

Fig. 3.18: Horizontal hitch beam with seat and support wheel

Fig. 3.19: Gear arrangement of rotary transmission system

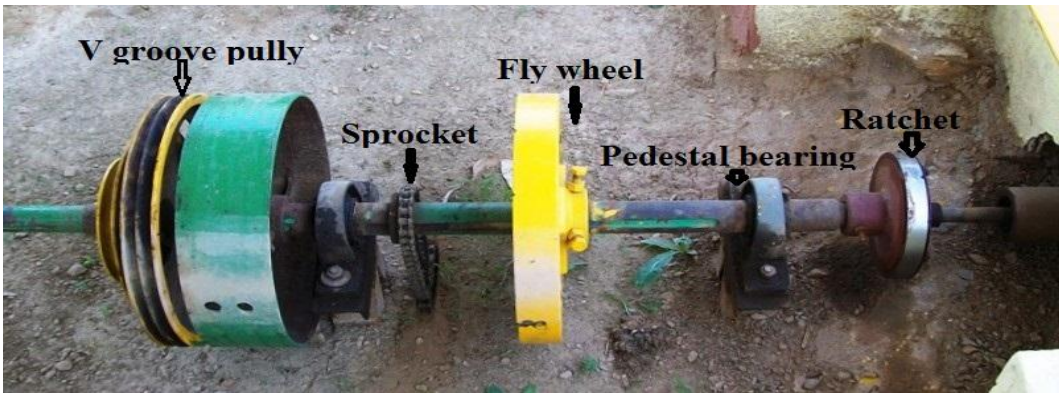

Fig. 3.20: Power output shaft of rotary transmission system

3.7.3 Test camel

A test camel in the age group of 9-10 years of Bikaneri breed was used for the experiments. The weight of camel was 550 kg. The accuracy and quality of work performed by an animal, depends upon training, regular practice and an effective guidance. The test camel was reluctant to operate in rotary motion initially, that reacted adversely and it became very difficult to handle them. Therefore, it had to be trained by a very skilled stockman or operator under whom they could be controlled. Trainer used a stick lightly on their hindquarters to encourage camel to follow the correct path until it became familiar with it. The path followed was also not a perfect circle. After training, the camel became accustomed to the pattern of the experiment and its strange behaviour was largely disappeared. The camel was fed fodder and fed daily as per recommended practice. The weight of the camel was regularly recorded. The health of animal was good throughout the experimental period.

3.8 Performance evaluation of matching gadgets in rotary mode of operation:

Through laboratory trials of four selected gadgets the shaft speed (rpm) and other parameter were standardized. By using proper sized pulley actual rpm was attained for selected gadgets in rotary mode. Selected gadgets were fixed on the MS railings and connected to the power output shaft of the rotary transmission system through V-belt and pulley.

In rotary mode the most important observations were animal physiological and physical parameters. Animal physiological and physical parameters were totally dependent upon the draught which acted upon the animal. According to the laboratory trials of electricity generation for battery charging required more power for a large span of time. Similarly in rotary mode condition for operating the electricity generation gadget create more draught upon the camel. For efficient working of camel fatigue score was used to indicate comparative stage of fatigue of camel. Depending upon this fatigue score a work-rest cycle was followed for battery charging.

Groundnut decorticator and maize dehusker cum sheller were creating comparatively low draught, similar to the laboratory simulation setup. For these two gadgets continuous sustained working time of camel was calculated on the basis of fatigue score. For calculation of fatigue score for continuous sustained working the simulating load was attached with the rotary mode transmission shaft by using CIAE animal loading car.

Fig. 3.21: Hitching arrangement for camel

Fig. 3.22: Telescopic shaft with universal coupling

Fig. 3.23: General view of rotary transmission system

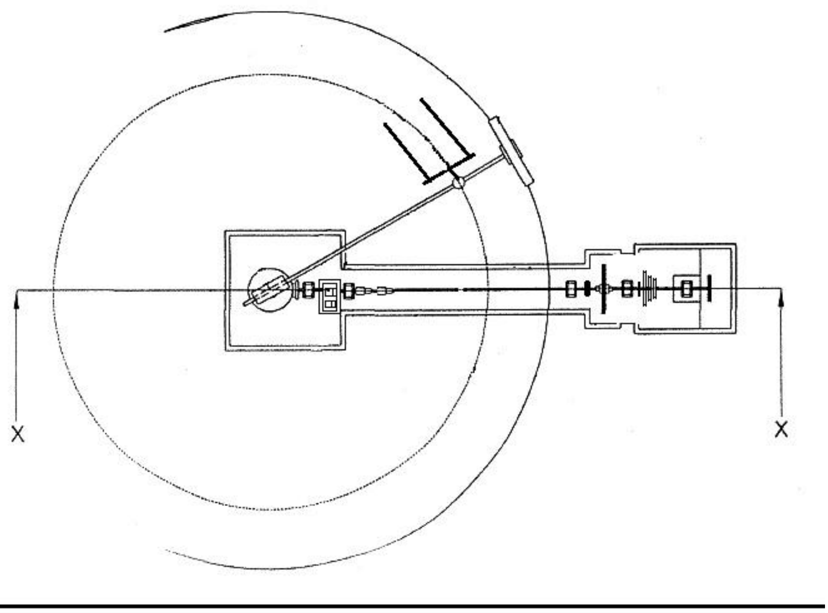

Fig. 3.24: Schematic diagram of camel powered rotary mode transmission system

3.8.1 Performance evaluation of electricity generation for battery charging by camel powered rotary transmission system

The laboratory experiment was conducted for charging two different Ampere-hour (Ah) batteries. It was found that the power requirement for 35Ah, 12 volt battery was close to the power generated by a camel thus a battery of 35Ah, 12 volt was selected for determining battery charging characteristics with developed rotary power transmission system. Alternator mounted on an MS frame was fixed on the MS railings and connected to the power output shaft of the rotary transmission system through V-belt and pulley (Fig. 3.25). Output of the alternator was connected to the battery through output variable panel. A camel was engaged to operate the rotary power transmission system. Physiological responses, draught requirement, speed of operation and battery charging parameters were recorded at regular intervals.

3.8.2 Performance evaluation of maize dehusker sheller in rotary transmission system

According to the laboratory trial the drum speed of 400 rpm was selected in rotary mode condition. Maize dehusker sheller mounted on a MS frame was fixed on the MS railings and connected to the power output shaft of the rotary transmission system through V-belt and pulley (Fig. 3.26). Pulleys were selected for getting 400 rpm of drum speed. Machine performance parameters and draught requirement were recorded during testing.

3.8.3 Performance evaluation of groundnut decorticator in rotary transmission system

Through laboratory simulation trial different parameters were standardized. According to this 300 rpm was selected for the drum speed. The groundnut decorticator was fixed on the MS railings and connected to the power output shaft of the rotary transmission system through V-belt and pulley (Fig.3.27). Pulleys were selected for getting 300 rpm of drum speed.

3.8.4 Performance evaluation of air compressor in rotary transmission system

From the laboratory simulation trials it was observed that at higher pressure range the load requirement of the air compressor became excessively more. But within few minutes air compressor reached its threshold point of air storage. According to all laboratory parameters 250 rpm speed was selected for crank shaft speed. Air compressor was fixed on the MS railings and connected to the power output shaft of the rotary transmission system through V-belt and pulley (Fig.3.28). Pulleys were selected for getting 250 rpm for crank speed.

Fig. 3.25: Testing of electricity generator in rotary transmission system

Fig. 3.26: Testing of maize dehusker sheller in rotary transmission system

Fig. 3.27: Testing of groundnut decorticator in rotary transmission system

Fig. 3.28: Testing of air compressor in rotary transmission system

3.9 Measurement of operating, physical and physiological parameters of camel:

3.9.1 Pull

A load cell of 500kgf mounted on the horizontal hitch beam was used to measure the pull [Fig.3.29 (a)]. It was connected between the hitch-beam and harness with the help of rod assembly**.** Through this system the pull was measured directly through the load indicator.

3.9.2 Speed

The test camel was allowed to travel five rounds of the test track at different conditions. The time for the same was recorded using a stopwatch. The travel speed in rpm was calculated from the recorded data and corresponding linear speed was calculated.

3.9.3 Pulse rate

Pulse rate was measured by placing the index or second finger on the coccigeal artery beneath the tail of camel and the number of beats per minute was counted [Fig.3.29 (b)]**.** The pulse rate was measured at the start of work and at suitable interval.

3.9.4 Respiration rate

The respiration rate was measured by counting the number of hot gushes exhaled per minute by placing the palm of hand near the nostrils of the camel [Fig.3.29 (c)]**.** The respiration rate was measured at the start of work and thereafter every suitable interval of work.

3.9.5 Body temperature

The body temperature of the camel was measured by inserting the clinical thermometer 40 to 50 mm inside of the rectum of camel for two minute duration [Fig. 3.29 (d)]**.** The body temperature was measured at the start of work and thereafter every suitable interval of work.

3.9.6 Physical symptoms

In addition to physiological parameters, physical symptoms such as frothing, tongue protrusion, excitement and leg un-coordination were also observed to access the fatigue in camel.

3.10 Fatigue Score Card

A fatigue score card suggested by Bhatt *et al.* (2002) was used to indicate comparative stage of fatigue of camel (Table. 3.2). The score card was based on total seven parameters on four point scale. The total fatigue score would be 28 from this score card. However, for deciding the fatigue

Fig. 3.29: Measurement of draught, respiration rate, pulse rate and body temparature of camel

score limit 21 point score had been considered as a safer limit for working of camels at different draught levels. Further this score card had been divided in four zones i.e. less tired, tired, more tired and excessive tired with their respective fatigue score of 0-7, 7-14, 14-21 and 21-28.

Table 3.2: Fatigue score card for camel

S. No.	Score	Less tired	Tired	More tired	Excessive tired
	Parameter	**1**	**2**	**3**	**4**
1.	PR (beats/min)	$P_0 + 5$	$P_0 +10$	$P_0 + 14$	$P_0 +17$
2.	RR (breaths/min)	$R_0 + 2$	$R_0 + 4$	$R_0 + 5$	$R_0 +6$
3.	BT/(RT) (^{0}C)	$T_0 +0.5$	$T_0 + 1.0$	$T_0 + 1.3$	$T_0 + 1.5$
4.	Speed (kmph)	S_0 - 0.1	S_0 - 0.2	S_0 -0.3	S_0.0.4
5.	Frothing	First appearing of frothing	Occasional falling of froth	Continuous falling from froth	Heavy frothing from mouth
6.	Water from eyes and nostrils	Appearance of water from nostrils	Occasional watering from nostrils and appearance of tears	Frequently appearance of water from nostrils and tears from eyes	Continuous flow of water from nostrils and tear from eyes
7.	Leg in coordination	Occasional dragging of feet	Frequent dragging of feet	No coordination between fore and hind legs	Staggered walking

P_0 = Pulse rate in zeroth hour of operation.

R_0 = Respiration rate in zeroth hour of operation.

T_0 = Body temperature/ Rectal temperature in zeroth hour of operation.

3.11 Simulation with animal loading car

CIAE loading car was used to apply load on the camel and the different physical and physiological parameters of camel for continuous working were observed at equivalent draught of maize dehusker sheller and groundnut decorticator. Both the machines required same range of draught of 55 to 60 kgf, which is about 10 to 10.9 per cent of draught with respect to camel's body weight. The loading car was set for the draught of 11 per cent of camel's body weight for rotary mode of operation. Fig.3.30 denotes schematic diagram of CIAE loading car.

It consisted of fluid tank, hydraulic pump, control valve and drive system. The drive from the output shaft was taken through chain and sprocket and connected to the loading device. The speed range of hydraulic pump was 180-900 rpm. The system has been designed to exert pressure in the range of 50 to 100 N/ cm^2. The flow of oil from hydraulic pump was restricted with the help of a valve to obtain the desired load. Details of the hydraulic system of the animal loading car are given in Appendix A.

Load car was attached with the help of chain sprocket (Fig. 3.31) to the output shaft of the rotary transmission system. The load was fixed according to the draught requirement of the gadgets and camel was allowed to operate in the sustained working condition. Physical and physical parameters of camel were recorded at regular interval for calculating the fatigue score.

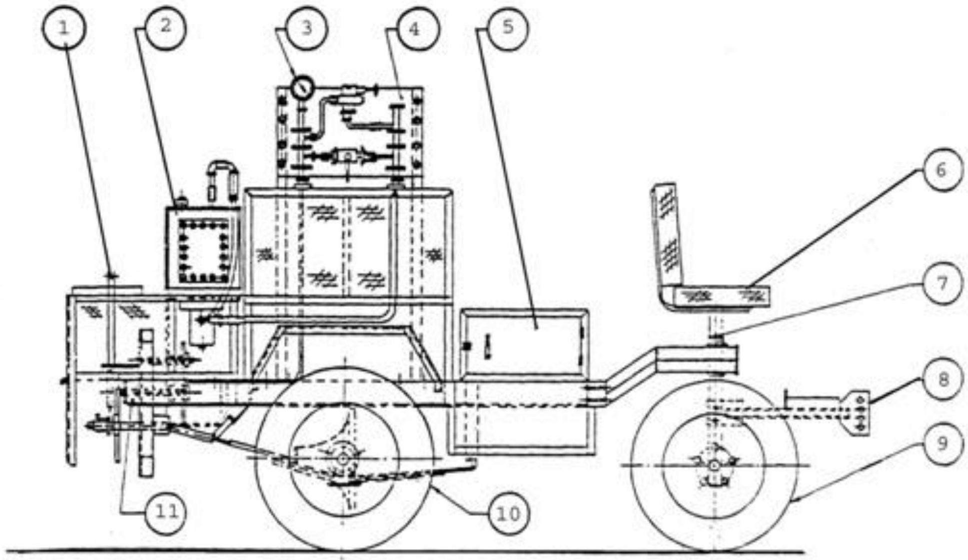

1, Lever to disengage drive during transport; 2, oil tank; 3, pressure guage; 4, control panel; 5, tool box; 6, seat; 7, front wheel turn table shaft; 8, hitch point; 9, front wheel; 10, rear wheel; 11, gear pump

Fig. 3.30: Schematic diagram of animal loading car

Fig. 3.31: Loading car for imparting load